Supplementary Information

Tumour suppression by targeted intravenous non-viral CRISPRa using dendritic polymers

J. A. Kretzmann, C. W. Evans, C. Moses, A. Sorolla, A. L. Kretzmann, E. Wang, D. Ho, M. J. Hackett, B. F. Dessauvagie, N. Smith, A. D. Redfern, C. Waryah, M. Norret, K. Swaminathan Iyer*, P. Blancafort*

* swaminatha.iyer@uwa.edu.au , pilar.blancafort@uwa.edu.au,

1 Methods 3
1.1 Polymer Synthesis and Characterization 3
1.1.1 Copolymer backbone 3
1.1.2 Click reaction 4
1.1.3 Fluorination 5
1.1.4 Non-targeted formulation 5
1.1.5 Targeted formulation 6
1.1.6 DLS and Zeta 7
1.1.7 CRISPR design and preparation 7
1.2 *In vitro* experiments 8
1.2.1 Cell culture (MCF-7, MCF-7-luc, H157) 8
1.2.2 Transfection 8
1.2.3 RNA extraction and PCR 8
1.2.4 Cell viability assay 10
1.2.5 Migration assay 10
1.2.6 Soft agar assay 11
1.3 BALB/c nude mice *in vivo* experiments 11
1.3.1 Ethics statement 11
1.3.2 Tumour inoculation and maintenance 11
1.3.3 Biodistribution experiment (inj, *in vivo* and *ex vivo* imaging, confocal) 11
1.3.4 Intravenous experiment (inj, imaging) 12
1.3.5 Bioluminescence imaging 13
1.3.6 Sectioning and staining (H&E, immunofluorescence) 13
1.3.7 Imaging 14
1.3.8 Statistical analysis 14
1.4 References 14

2 Supplemental Data 16
2.1 MASPIN and CCN6 expression in normal breast tissue 16
2.2 Polymer structure and characterization 19
2.3 Gene regulation in H157 cells 21
2.4 Off-target analysis 21

2.5	Soft agar assay	22
2.6	DLS and zeta	22
2.7	In vitro transfection of targeted polymer formulation	23
2.8	Fluorescent spectral characterisation	23
2.9	Biodistribution	24
2.10	Tumour growth	27
2.11	Histology	29
2.12	Tissue IF	33

1 Methods

1.1 Polymer Synthesis and Characterization

All chemicals were purchased from Sigma Aldrich (Australia) and used without further purification unless otherwise stated. Cyanine7 NHS ester (Cy7-NHS) was purchased from Lumiprobe. Peptides (H-DfC(1230)RG-cyclic, 99% purity **14** and H-DfC(51)RG-cyclic, 97% purity **13**) were custom designed and synthesized by Mimotopes (Melbourne, Australia). $SM(PEG)_{12}$ (Thermo Scientific, 100 mg) was diluted by adding 360 µL of dry DMSO, as per manufacturer's protocol, and stored under argon at –20 °C.

^{1}H and ^{19}F NMR spectra were measured using a Bruker Avance AV500 spectrometer (500 MHz), using CD_3OD as the solvent for copolymers, aminated copolymers, dendronized polymers and fluorinated compounds. The chemical shifts were referenced to the solvent peak, δ = 3.31 ppm for CD_3OD. For ^{19}F spectra, hexafluorobenzene was used as a standard, with a chemical shift of δ = -164.9 ppm. IR spectra were obtained using a PerkinElmer Spectrum One FT-IR spectrometer. Gel permeation chromatography (GPC) was used to determine the molecular weight and polydispersity index of polymers (Waters Styragel HR 4 DMF 4.6 × 300 mm column, 5 µm). Agilent Technologies 1100 Series GPC and Agilent GPC software were used for measurements and data analysis respectively. Measurements were taken using DMF as the eluent at a flow rate of 0.3 mL/min at 50 °C, and calibrated against poly(methyl methacrylate) (PMMA) standard. Elemental analysis was conducted by the Campbell Microanalytical Laboratory at the University of Otago, New Zealand.

1.1.1 Copolymer backbone

Scheme S1. Synthesis of p(PHEMA$_{0.84}$-*ran*-GMA$_{0.16}$) copolymer.

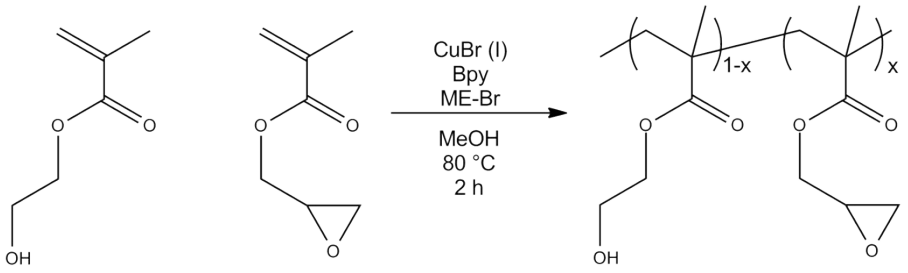

P(HEMA$_{0.84}$-*ran*-GMA$_{0.16}$) copolymer was synthesized as previously described,[1] adapted from Weaver *et al.*[2] Briefly, inhibitors for hydroxyethyl methacrylate (HEMA, **1**, 7.5 mmol) and glycidyl methacrylate (GMA, **2**, 24.7 mmol) were removed *via* passage through a plug of basic alumina and reacted using an atom-transfer radical polymerization method to afford copolymer **3**. Copolymer composition was determined by ^{1}H NMR (500 MHz, CD_3OD), where integration of peaks δH 2.70 (1H, br) and 2.87 (1H, br) corresponding to the epoxide moiety was used to determine copolymer consists of 16.3 mol% GMA **2**. Polymer molecular weight (21.5 kDa) and PDI (1.30) of the polymer measured using GPC.

1.1.2 Click reaction

Scheme S2. Synthesis of dendronised polymer via copper-catalyzed click reaction.

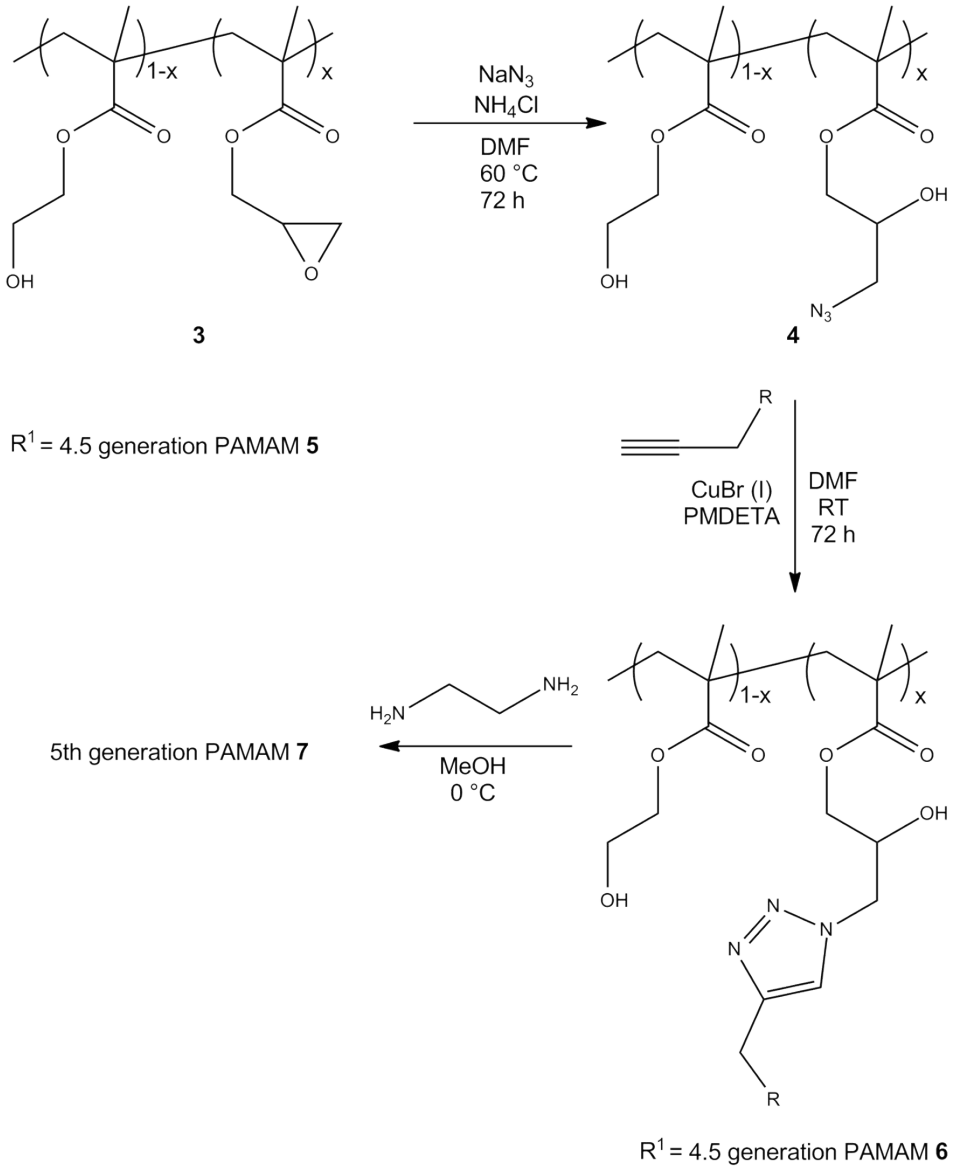

Azido functionalization: Copolymer **3** was functionalized with azido groups as described previously, to afford product **4**.[1]

Propargyl dendron synthesis: 4.5 generation (G4.5) propargyl PAMAM dendron **5** was synthesized using methods adapted by Lee *et al.*[3] and Lin *et al.*[4]

Click reaction: Propargyl poly(amido amine) dendrons were attached via an azide-alkyne click reaction to afford product **6** and generation finalized to G5 by reaction with ethylene diamine, resulting in final product **7** as previously described,[1] adapted from Zhao *et al.*[5]

1.1.3 Fluorination

Scheme S3. Functionalization of surface primary amines with heptafluorobutyric anhydride.

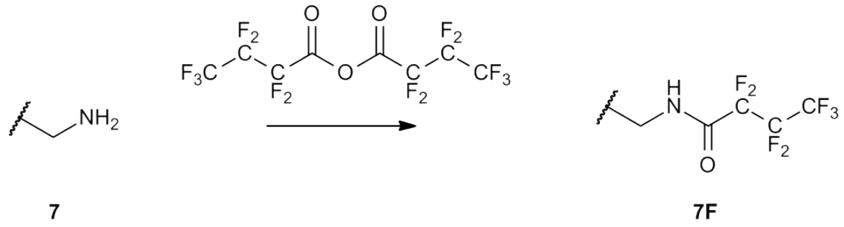

7 **7F**

Polymer **7** (104 mg) was fluorinated by reaction with heptafluorobutyric anhydride (91.3 µL, 0.37 mmol), resulting in fluorinated polymer **7F**, as per protocol described by Wang *et al.*[6]

1.1.4 Non-targeted formulation

Scheme S4. Surface functionalization for non-targeted in vivo formulation.

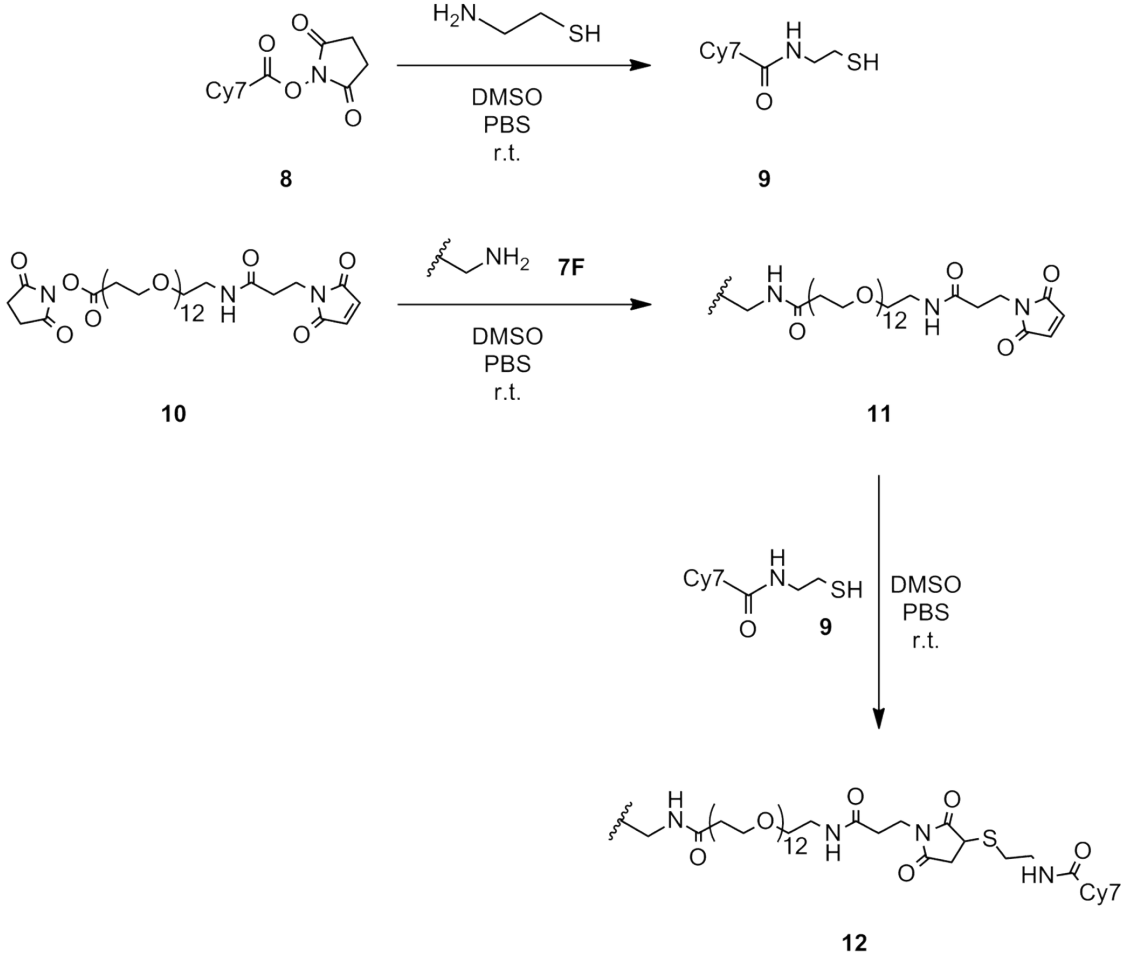

8 **9** **10** **11** **12**

Cy7-NHS (**8**, 0.55 mg, 0.81 µmol) was dissolved in 50 µL of DMSO, and added to cysteamine solution in PBS (phosphate buffered saline solution, 62.2 µL, 1 mg/mL, 8.06×10^{-7} mol). 200 uL of extra PBS was added and pH adjusted to 8. Reaction was left to proceed at r.t. for 2 h. Polymer (**7F** 10.2 mg, 19.6

µmol primary amines) was dissolved in 0.5 mL PBS, and SM(PEG)$_{12}$ **10** DMSO solution (2.5 µL) was added. pH was adjusted to 7 and reaction was left to proceed at r.t. for 2 h. Reaction mixtures were combined and left to react at pH 7 and r.t. overnight. Product **12** was purified by dialysis (membrane MW cutoff 12–14 kDa) in PBS followed by deionized water, and collected by lyophilization. Reaction was confirmed by spectral characterization (Varian Cary Eclipse fluorescence spectrophotometer).

1.1.5 Targeted formulation

Scheme S5. Custom RGD targeting peptides used in in vivo targeting formulation.

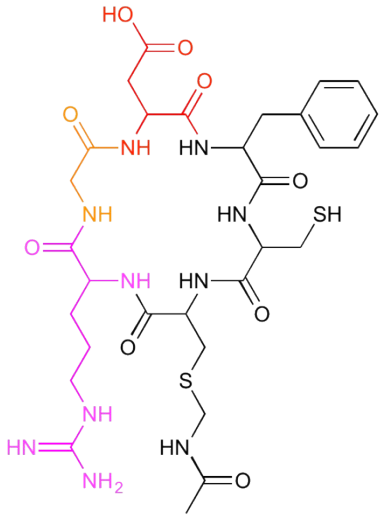

13

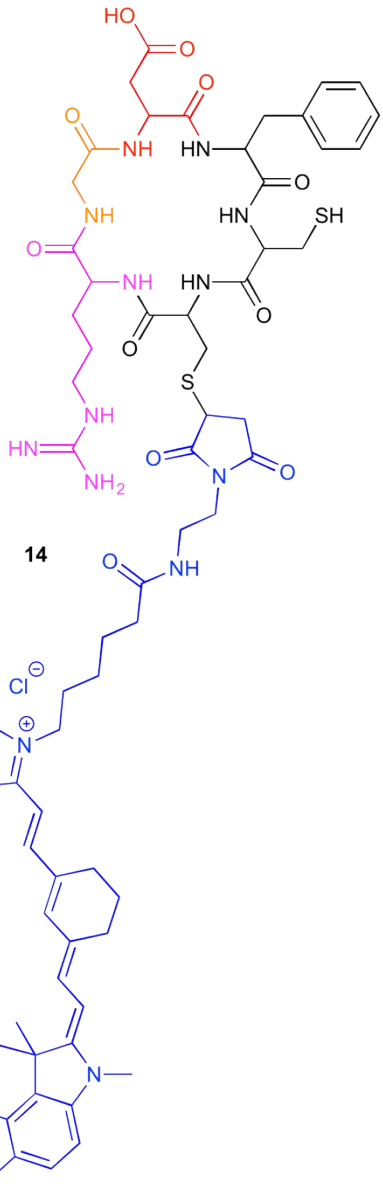

14

Scheme S6. Surface functionalization for targeted *in vivo* formulation.

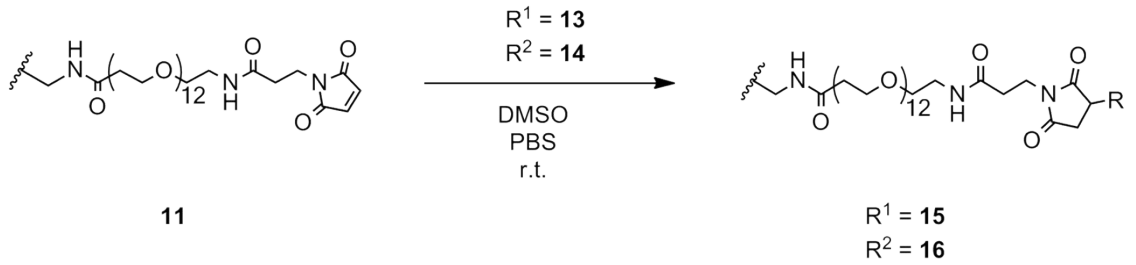

Polymer (**7F**, 8.7 mg, 16.7 µmol primary amines) was dissolved in 400 uL of PBS and reacted with SM(PEG)$_{12}$ **10** DMSO solution (2.19 µL) at r.t. for 2 h at pH 7, to give **11**. Peptide H-DfC(1230)RG-cyclic **14** (1.0 mg, 0.67 µmol) was dissolved in 300 µL of PBS and added to the stirring reaction mixture. Reaction was left to proceed overnight at r.t., pH 7, and product purified by dialysis (membrane MW cutoff 12–14 kDa) in PBS followed by deionized water, and collected by lyophilization. Product **16** was confirmed by spectral characterization. Formulation without Cy7 (reaction with **13** to give product **15**) was prepared by same protocol and reaction was confirmed by ^{1}H NMR (500 MHz, CD_3OD), where the appearance of peak δH 3.78 corresponds to the PEG functionalisation.

1.1.6 DLS and Zeta

Polymer solutions were mixed with pDNA at appropriate N/P ratios and incubated at room temperature for 30 min in PBS. Size and zeta potential of the resulting polyplexes were characterized using dynamic light scattering (Zetasizer Nano ZS), using a 4 mW He-Ne laser operating at 633 nm with a scattering angle of 173°. Measurements were taken in triplicate after an initial equilibration period of 2 min. For calibration of the measurements 'material' was defined as PGMA (refractive index of 1.515 and absorbance of 0.05) and 'dispersant' was defined as water at 25 °C (refractive index of 1.330 and viscosity of 0.887). The intensity-weighted zeta potential and hydrodynamic radius of the polyplexes is presented as mean ± standard deviation. All zeta potential measurements were taken at pH ≈ 7.4.

1.1.7 CRISPR design and preparation

All dCas9 constructs used an inactivated form of *S. pyogenes* Cas9 protein with two mutations in D10A and H840A. pcDNA-dCas9-No effector (Addgene plasmid #47106) was a gift from Charles Gersbach. pcDNA-dCas9-VPR with VP64, p65 and Rta fused to its C-terminus (Addgene plasmid #63798) was a gift from George Church. MS2-P65-HSF1_GFP (Addgene plasmid #61423), expressing the SAM helper complex with a 2A GFP, was a gift from Feng Zhang. The Benchling CRISPR design tool was used to select sgRNA target sequences in the *MASPIN* and *CCN6* proximal promoters. Annealed oligonucleotides (Integrated DNA Technologies, Singapore) containing the sgRNA target sequences were cloned into BbsI sites in the sgRNA(MS2) cloning backbone (Plasmid #61424), which was a gift from Feng Zhang. Plasmids were prepared using the QIAGEN Plasmid Maxi Kit (QIAGEN).

1.2 *In vitro* experiments

1.2.1 Cell culture (MCF-7, MCF-7-luc, H157)

MCF-7 and MCF-7 luciferase (human breast adenocarcinoma cell line, ATCC, and MCF-7 modified in-house to express luciferase) were cultured in Minimum Essential Medium α (MEM α, Gibco) supplemented with 0.15% sodium bicarbonate, 10% FBS and 1× GlutaMAX. H157 (human lung adenocarcinoma cell, ATCC) were cultured in RPMI1640 supplemented with 10% FBS and 1× GlutaMAX. All cell lines were grown in a humidified incubator at 37 °C with 5% CO_2. Cell lines were seeded in 12-well plates (Corning Costar, Sigma Aldrich) in media without antibiotic/antimycotic for *in vitro* experiments. Cell seeding densities are summarized in Table S1.

Table S1. Seeding densities for transfection experiments in a 12-well standard culture plate

Cell line	Seeding density (cells/mL)
MCF-7	1.8×10^5
H157	1.0×10^5

1.2.2 Transfection

Transfections were performed as described previously.[1] Briefly, polymer solution and pDNA were diluted to the required concentration in Opti-MEM reduced serum media (Gibco). For a 12-well standard plate format, polymer solution was prepared as 5 mM primary amines in filtered sterilised Milli-Q water, and 2.4 µL of polymer solution was diluted to a total 70 µL in Opti-MEM. 1 µg of pDNA (in 70 µL of Opti-MEM) was then mixed thoroughly with the polymer preparation, and then incubated for 30 min at r.t. 130 µL of the polyplex solution was then transferred to the appropriate well, which had been washed twice with phosphate buffered saline solution (PBS) and 300 µL of Opti-MEM added. After a 4 h incubation period, an additional 570 µL of the appropriate complete culture medium was added and the experiment incubated for a further 44–68 h, giving a total transfection time of either 48 h or 72 h, respectively for RNA extraction and downstream assays. Cells were harvested for downstream assays at 48 h after transfection.

1.2.3 RNA extraction and PCR

In vitro experiments

Total RNA was extracted using 1 ml Trizol reagent (Invitrogen) for approximately 1×10^7 cells, according to the manufacturer's protocol. Extracted total RNA was converted to cDNA using the High Capacity cDNA Reverse Transcription Kit (4368813, Applied Biosystems). The expression levels of the gene of interest were analysed with real-time reverse transcription quantitative PCR (RT-qPCR) with *GAPDH* as housekeeping control. RT-qPCR was carried out using TaqMan Fast Universal PCR Master Mix (4352042, Applied Biosystems). Primer-probe set sequences used to detect mRNA levels were commercially purchased as detailed in Table S2. For additional off target analysis, RT^2 SYBR Green ROX qPCR Mastermix was used (330521, Qiagen), primer-probe set sequences used to detect mRNA levels were designed in-house and commercially purchased, as detailed in Table S3.

Table S2. Primer-probe set information for TaqMan mRNA analysis.

Target	Catalogue number	Supplier
GAPDH	4332649	Applied Biosystems
MASPIN	Hs00985285_m1	Thermo Fisher
CCN6	Hs00180236_m1	Thermo Fisher
LMX1A	Hs00898455_m1	Thermo Fisher
CFAP52	Hs00376807_m1	Thermo Fisher
CDC123	Hs00990152_m1	Thermo Fisher
NXNL2	Hs00708156_s1	Thermo Fisher

Table S3. Primer-probe set information for SYBR green mRNA analysis.

Target	Sequence (5' to 3')	Supplier
MROH6	Forward: CCA CCC TGA TGG TGA CAG AG Reverse: AAT GGG GTG AGG GAT GAG GA	Integrated DNA Technologies
TMEM273	Forward: AGA GCC CCA AGA AAG CTG CAA Reverse: CCT CTT CAC GTC ACT GCT CAC	Integrated DNA Technologies
TMEM189	Forward: GGG GCT CTC ATT GCT GAC TT Reverse: GGA TGA AAG CCT TCC CCA CA	Integrated DNA Technologies
NPM2	Forward: TAG CCG TGC TCC TCA GTG TG Reverse: CGT TT TCC AGC CTA CCG TG	Integrated DNA Technologies
RASGRF2	Forward: CCT GTA CCT GGC CTT TCT GG Reverse: CCT CGG CCG TCT TCT TAC TC	Integrated DNA Technologies
ATF3	Forward: TGG CAA CAC GGA GTA AAC GA Reverse: GCA TCA TTT TGC TCC AGG CTC	Integrated DNA Technologies
KIAA	Forward: CAT GTC CCT GCA GAC CGT Reverse: GGC ACA GAA ACT CCA GGG G	Integrated DNA Technologies
ZNF620	Forward: ACC CAG AAT GAA TGG GCC AG Reverse: GTG AAT GGG AAT GCC AGG GA	Integrated DNA Technologies
PSMC2	Forward: CCA AAA ACC AGC GTG CCA AA Reverse: ACA CAG CAC CTT CCT TGC TT	Integrated DNA Technologies
OSBP2	Forward: TCC AAA GTC AAG AGG CGA GT Reverse: GTC CAG CAG GTG GTG GTA CT	Integrated DNA Technologies
EMP1	Forward: GCC AGT GAA GAT GCC CTC AA Reverse: ATA GCC GTG GTG ATA CTG CG	Integrated DNA Technologies
SARDH	Forward: GAA CTT GGG CCA CAC TCC TT Reverse: TAT GGC ACA CTC TCC TCG GC	Integrated DNA Technologies
ITGA7	Forward: ACC AAT ACC CTG ACC TGC TG Reverse: CTA TAG CTG CTG GGG ACT GC	Integrated DNA Technologies
LMNA	Forward: TTG ACC CGA GGA GGA TAG GG Reverse: CCA TCC CAC TCC TAG CTT GC	Integrated DNA Technologies
NBEA	Forward: ACC CGG CTA ATT AAT CCC CAC Reverse: CTA CTC CAA CCC GAG GCA AG	Integrated DNA Technologies
NAB1	Forward: GTG GGA CAT ACA AGC GTT GG Reverse: GAA CGA CCA CTC GGA GTC TG	Integrated DNA Technologies
DNAJC2	Forward: CGG AAG TGC TTA CTG GTC GT Reverse: ACA GAG TGT AGA GGC AGA GGT	Integrated DNA Technologies
PTPRR	Forward: TAA GAC CCG GAG AAG CGG AA Reverse: GTA GGA GGT TGC GGG TAA GG	Integrated DNA Technologies
USP31	Forward: AAC TCG GTC CAA AAG CCA CA Reverse: GAG CTC TTC GCC GAG TAC C	Integrated DNA Technologies
EXT1	Forward: CGT GCC TCT TTG TCC TGA GT Reverse: ATG TCA AAC CCC ACG TCC TC	Integrated DNA Technologies
VEZT	Forward: CCT GTT AAA AGT GGC TGA AAC CAT	Integrated DNA Technologies

	Reverse: CCA GGG AGC AAA GTG TTG GA	
HIGD2A	Forward: AAC CAT CGA AGC CTC CAG TC Reverse: TGG AAG GAG TAG AGG CCG TA	Integrated DNA Technologies
LINGO2	Forward: GGA GCT TAA AGA CAC AAA CGG G Reverse: CTT TCG GTG CTC TGC TCT GA	Integrated DNA Technologies
ATRIP	Forward: AGC TTT GCA AGA AAG CAG ACA C Reverse: TGT CAC TGA GTG CTT GGG TTT	Integrated DNA Technologies
SHISA5	Forward: TGG CTG CTG CTG CTA ACG Reverse: AAG GTT GTT CAG GCA AGG AG	Integrated DNA Technologies
SPIRE1	Forward: TGG TGA TAT TCC CCC TCG GT Reverse: GTG GCC GCA TTG CTA ATC TG	Integrated DNA Technologies
ZNF800	Forward: GTG ATG TAC GAA AAG GTT TGG AGT Reverse: GCA CAA GGT CAA GGG TGG AT	Integrated DNA Technologies
NIPAL2	Forward: CCC AGA GAG AAA GGC TTG GA Reverse: GGA AGT CCC CGA TGG TCC AT	Integrated DNA Technologies
FGD6	Forward: CGG GAG TCA TCA TCT CAG GC Reverse: TTT GCA TCA GCG TCC TCC AT	Integrated DNA Technologies
NOP16	Forward: GCC TGG GAC CAC GCT AAA TC Reverse: GGA AGT CTT GCC ACT CTG CTT AT	Integrated DNA Technologies
CACNA1C	Forward: TTT CAA ATG GTG TAG CCG CC Reverse: CTT TCG CGC AAG ATT CGA GG	Integrated DNA Technologies
PHC3	Forward: GTA TGC AGC CCA ACA ACA GC Reverse: GAA GCC TGG GAA CGG CTT AT	Integrated DNA Technologies
TREX1	Forward: TAC CTA CCC AAC CAT GGG C Reverse: TGC TCA GAC CTG TGA TCT CG	Integrated DNA Technologies
CMSS1	Forward: CCT ACC CGT GAT GTT CTG CC Reverse: GTT CTC CCA CCA CTC GTC TC	Integrated DNA Technologies
INHBA	Forward: GCT CAG ACA GCT CTT ACC ACA Reverse: CCT CTC AGC CAA AGC AAG GG	Integrated DNA Technologies
YIPF5	Forward: GCG CAG CCT CAG AGT TTG ATT Reverse: GCT ATA GGG TCC TCC ACT TCC TC	Integrated DNA Technologies

Analysis was performed in the ViiA 7 Real-Time PCR System (Applied Biosystems) and analyzed using QuantStudio Real Time PCR Software (v1.1, Applied Biosystems). Data were analyzed according to MIQE guidelines and results are expressed as fold change compared to dCas9 No Effector transfected cells after normalization against *GAPDH* mRNA levels.

1.2.4 Cell viability assay

Cell viability assay was carried out in 96-well flat-bottom tissue culture plates at a seeding density of 2.5×10^4 cells/well and was added to each well. Plates were incubated at 37 °C in a 5% CO_2 atmosphere for 48–120 h and were quantified with CellTiter-Glo reagent (Promega) according to the manufacturer's protocol, except that only 10 µl reagent was added to each well. This has been previously confirmed to still give a linear response with cell density.[1] Luminescence was measured using EnVision 2102 Multilabel reader (PerkinElmer).

1.2.5 Migration assay

Comparative migration assay was performed as per manufacturer's protocol (CytoSelect Migration Assay, 8 µm, colorimetric format, Cell Biolabs, Inc.). Briefly, cells were transfected 48 h prior to being collected and resuspended in serum free media for counting and seeding. Cells were seeded at 0.75×10^6 cells (in 500 µL) in upper chamber without serum. Full growth media was added below the

chamber to encourage cell migration through the polycarbonate membrane. After 24 h cells were stained as per protocol, lysed, and the lysate absorbance quantified using EnVision 2102 Multilabel reader (PerkinElmer).

1.2.6 Soft agar assay

For soft agar assay, cells were transfected for 48 h, then harvested and counted. 5000 cells per well were seeded on a 6 well plate with growth medium, plated on top of a solidified layer of 0.5% agarose in growth medium and below a 0.35% agarose in growth medium and fed every 3 days with growth medium. After 3 weeks, the colonies were imaged by digital camera (Olympus). Conditions were analyzed in triplicate, with 6 fields of view marked at day 1 and imaged at 3 weeks for growth assessment. ImageJ software was used to assess the number and diameters of colonies.

1.3 BALB/c nude mice *in vivo* experiments

1.3.1 Ethics statement

A power analysis was performed prior to our *in vivo* studies. The power analysis was based on a study using a nanoparticle formulation of a chemotherapeutic delivered, to a similar MCF-7 xenograft model in nude mice.[7] Using the reported results as the "expected" values (~75% difference in tumour size with ~± 25% s.d), the power analysis suggested that n = 3 was the optimal number of animals needed to obtain statistical significance.

Normal human breast tissues used as positive controls from staining protocols were taken from the de-identified control tissue archive routinely used by PathWest to provide validatory controls as part of routine clinical practice.

1.3.2 Tumour inoculation and maintenance

MCF-7-luciferase (MCF-7-luc) cells were cultured routinely as described above. For tumour inoculation, cells were collected and resuspended in 50:50 mixture of MEM α and Matrigel (Corning BD Bioscience 354248), with 1 µg estrogen (β-Estradiol 17-valerate, Sigma Aldrich E1631). Animals were injected in right flank with cell suspension (5 x 10^6 cells/animal, 60 µL). Tumours were maintained by subcutaneous injections of estrogen (20 µL, 50 ng/µL in peanut oil) located near the periphery of the visible tumour every 48 h. Animals were humanely sacrificed prior the end of experiment date, or removed from the study for the following reasons: tumour burden exceeding ethics protocol, hypoxic (pitting) tumours, tumours growing within the peritoneal layer (no longer xenograft model).

1.3.3 Biodistribution experiment (inj, *in vivo* and *ex vivo* imaging, confocal)

Tumours were inoculated and maintained as above. 7 days after tumour inoculation mice were randomly divided into two groups (N = 7 per group) and injected by a single intravenous injection containing either the targeted **16** or non-targeted polymer **12** formulation and mCherry plasmid (10 µg plasmid/injection, N/P = 5 for each polymer formulation). Animals (N = 3 per group) were anesthetized (isoflurane) and imaged using CRi Maestro 2 (740 nm to 950 nm, 10 nm step) at 24, 48 and 72 h timepoints, and culled at 72 h for *ex vivo* imaging of tissue. Additional animals (N = 2 per group, per timepoint) were culled at 24 and 48 h timepoints for *ex vivo* tissue imaging.

Tissue for sectioning and IF: Tissues were washed in PBS, snap frozen in OCT (Sakura Tissue-Tek) and stored at –80 °C prior to being sectioned at 8 µm thickness using a Leica cryostat. Samples were stained for mCherry as per the protocol below (section 1.3.6), with the additional steps of initial fixation in 2% paraformaldehyde (PFA) in PBS for 10 min, and hydration with mqH_2O for 5 min.

Tissue for sectioning and FTIR analysis: Tissues were washed in PBS, snap frozen in OCT (Sakura Tissue-Tek) and stored at –80 °C prior to being sectioned at 8 µm thickness using a Leica cryostat. Sections were melted onto an infrared transparent CaF_2 substrate (1 mm thick, 25 mm diameter, Crystran). Tissue sections were air-dried under ambient laboratory conditions, and stored in the dark in the presence of desiccant until analysis.[8,9]

A FTIR Spectroscopic Data Collection: FTIR microscopy was performed using a Nicolet iN 10MX FTIR microscope, equipped with a liquid nitrogen cooled 8×2 pixel linear array detector (25 µm effective pixel size). The FTIR images were acquired at 4 cm^{-1} spectral resolution and using co-addition of 16 scans. Images were collected at ambient laboratory temperature, under conditions of a dry-nitrogen purge. For each sample, a background image was collected using the same conditions from a region of blank substrate.

FTIR Spectroscopic Data Analysis: To generate functional group images of relative nucleic acid content and distribution, the FTIR spectra were analysed with Cytospec v2.00.03 and OPUS v7.0. Second-derivative spectra were generated from vector normalized raw spectra (vector normalized across amide I band from 1700 – 1600 cm^{-1}), using a 13 smoothing point Savitzky-Golay function. FTIR false colour images of nucleic acid distribution were generated from the second-derivative intensity at 1055 cm^{-1}, assigned to the nucleic acid ribose ν(C-O) mode.[10] Image masks were created from regions of interest around nucleic acid influx into the kidney tissue sections, to calculate an average nucleic acid content.

Flow cytometry: Flow cytometry was conducted using BD FACSCantoII flow cytometer and samples were acquired using BD FACS Diva software. 100,000 single cell events, gated on forward scatter area vs height were recorded for analysis. Viable cells (calcein-AM stained) were gated for using a 488 nm laser and emission measured using 505 nm long pass and 530/30 nm band pass filters; mCherry was excited by a 561 nm laser, and emission was measured with 595 nm long pass and 610/20 nm band pass filters; Cy7 was excited by a 640 nm laser and emission was collected with 750 nm long pass and 780/60 nm band pass filters. Cultured MCF-7 cells were used as positive controls for calcein-AM, mCherry and Cy7, and non-fluorescent tissue was used as a negative control.

1.3.4 Intravenous experiment (inj, imaging)

MCF-7-luc tumours were inoculated and maintained as described previously. Intravenous injections were given to mice (N = 11 per group) every 72 h, starting 7 days after tumour inoculation. Mice were injected with 'targeted' polymer formulation (**14**, 56.4 µg) and plasmid DNA (5 µg). Mice were treated with either pcDNA, dCas9 no effector, dCas9-VPR/SAM (MASPIN) or dCas9-VPR (CCN6) formulations. Mice received a total of 5 injections.

Tumour progression was followed by caliper measurements every 48 h. Mice were sacrificed at day 23, 39 and 46 (N = 3 per timepoint) for tissue collection and analysis.

1.3.5 Bioluminescence imaging

Mice received an intraperitoneal injection of D-luciferin (200 µL, 15 mg/mL in PBS) prior to being anesthetized (4% isoflurane initially, 2% to maintain state during imaging). Mice were imaged for bioluminescence using Caliper IVIS Lumina II imaging system 10–15 min after injection, once bioluminescence signal intensity had reached steady state.

1.3.6 Sectioning and staining (H&E, immunofluorescence)

Tissue was collected and preserved in 4% paraformaldehyde (PFA) in PBS. Prior to wax-embedding, tissue was washed and stored in 70% EtOH. 5 µm sections of collected tissue were cut using Leica wax microtome. Sections either underwent standard hematoxylin and eosin (H&E) staining, or were stained for immunofluorescence analysis.

Immunofluorescence staining: Tissue sections were dewaxed and hydrated as per standard protocol. Antigen retrieval was conducted using KOS Microwave Multifunctional Tissue Processer with samples in sodium citrate buffer (10 mM sodium citrate, 0.05% Tween-20, pH 6.0). Staining method was adapted from Abcam published ICC and IF protocol.[11] Briefly, tissue was permeabilized by incubation in 0.2% Triton X-100 in TBST (TBS, 0.1% Tween 20) for 10 min and then washed three times for 5 min with TBST. Sections were blocked with 1% BSA and 10% normal goat serum in TBST for 90 min at room temperature. Blocking solution was removed and tissue sections were incubated with primary antibody in 1% BSA in TBST at 4°C overnight in a humidified chamber. Primary antibody solution details can be found in Table S3.

Solution was decanted and sections washed three times in TBST for 5 min per wash, then incubated with secondary antibody (AF647-conjugated donkey anti-rabbit, 1:400, Abcam ab150075; or AF633-conjugated goat anti-rabbit, 1:400, Molecular Probes A-21070; or AF647-conjugated chicken anti-mouse, 1:400, Molecular Probes A-21463) in 1% BSA at r.t. for 1 h. Secondary antibody solution was removed, sections were washed three times in TBST for 5 min each and sections were incubated with Hoechst 34580 (Sigma Aldrich, 1:1000 dilution in TBST), washed three times in TBST for 5 min and mounted using Fluoromount-G aqueous mounting media (Southern Biotech).

Table S4. Primary antibody purchase and dilution details.

Target	Supplier	Catalogue Number	Dilution
Ki67	Cell Signaling Technology	9449S	1:400
CRISPR-Cas9	Abcam	Ab191468	1:200
Cleaved caspase 3	Cell Signaling Technology	9661S	1:300
MASPIN	BD Bioscience	554292	1:300
CCN6	Santa Cruz	sc-25443	1:300
mCherry	Abcam	ab167453	1:500

1.3.7 Imaging

Scanscope: H&E stained sections for histology were imaged at 20× magnification using a Leica (Aperio) Scanscope XT Digital Slide Scanner. Images were processed using Aperio ImageScope software.

Confocal: Sections were imaged using a Nikon Ti-E inverted confocal microscope. Images were collected using NIS-C Elements software and processed using ImageJ. Images were taken using a 20x

air objective (NA0.75), and sequential excitation using wavelengths of 405 nm (Hoechst 34580), 488 nm (autofluorescence) and 638 nm (AlexaFluor 647 secondary antibody).

The immunofluorescent assays were performed for n = 3 animals per time point, where 3 images/section were taken in a blinded study. To quantify, image coordinates were first chosen on a control image, and the same coordinates were then used to quantify positive cells (for HA, Ki67, CC3 and CRISPR/dCas9 stains) by counting, and MASPIN/CCN6 expression by fluorescent intensity.

1.3.8 Statistical analysis

Statistical analyses were performed with GraphPad Prism (GraphPad Software Inc.) The data is illustrated as the mean; error bars represent the standard deviation unless otherwise stated. For all tests, differences were considered significant at $p \leq 0.05$ (*), $p \leq 0.01$ (**), $p \leq 0.001$ (***), $p \leq 0.0001$ (****).

1.4 References

(1) Kretzmann, J. A.; Ho, D.; Evans, C. W.; Plani-Lam, J. H. C.; Garcia-Bloj, B.; Mohamed, A. E.; O'Mara, M. L.; Ford, E.; Tan, D. E. K.; Lister, R.; et al. Synthetically Controlling Dendrimer Flexibility Improves Delivery of Large Plasmid DNA. *Chem. Sci.* 2017, *8* (4), 2923–2930.

(2) Weaver, J. V. M.; Bannister, I.; Robinson, K. L.; Bories-Azeau, X.; Armes, S. P.; Smallridge, M.; McKenna, P. Stimulus-Responsive Water-Soluble Polymers Based on 2-Hydroxyethyl Methacrylate. *Macromolecules* 2004, *37* (7), 2395–2403.

(3) Lee, J. W.; Kim, B.-K.; Kim, H. J.; Han, S. C.; Shin, W. S.; Jin, S.-H. Convergent Synthesis of Symmetrical and Unsymmetrical PAMAM Dendrimers. *Macromolecules* 2006, *39* (6), 2418–2422.

(4) Lin, Y.-J.; Tsai, B.-K.; Tu, C.-J.; Jeng, J.; Chu, C.-C. Synthesis of β-Cyclodextrin and Poly(amido Amine) Dendron Click Cluster and Its Synergistic Binding Property. *Tetrahedron* 2013, *69* (7), 1801–1807.

(5) Zhao, P.; Yan, Y.; Feng, X.; Liu, L.; Wang, C.; Chen, Y. Highly Efficient Synthesis of Polymer Brushes with PEO and PCL as Side Chains via Click Chemistry. *Polymer* 2012, *53* (10), 1992–2000.

(6) Wang, M.; Liu, H.; Li, L.; Cheng, Y. A Fluorinated Dendrimer Achieves Excellent Gene Transfection Efficacy at Extremely Low Nitrogen to Phosphorus Ratios. *Nat. Commun.* 2014, *5*, 3053.

(7) Lee, E. S.; Na, K.; Bae, Y. H. Doxorubicin Loaded pH-Sensitive Polymeric Micelles for Reversal of Resistant MCF-7 Tumor. *J. Controlled Release* 2005, *103* (2), 405–418.

(8) Hackett, M. J.; Britz, C. J.; Paterson, P. G.; Nichol, H.; Pickering, I. J.; George, G. N. In Situ Biospectroscopic Investigation of Rapid Ischemic and Postmortem Induced Biochemical Alterations in the Rat Brain. *ACS Chem. Neurosci.* 2015, *6* (2), 226–238.

(9) Hackett, M. J.; McQuillan, J. A.; El-Assaad, F.; Aitken, J. B.; Levina, A.; Cohen, D. D.; Siegele, R.; Carter, E. A.; Grau, G. E.; Hunt, N. H.; et al. Chemical Alterations to Murine Brain Tissue Induced by Formalin Fixation: Implications for Biospectroscopic Imaging and Mapping Studies of Disease Pathogenesis. *Analyst* 2011, *136* (14), 2941–2952.

(10) R. Wood, B. The Importance of Hydration and DNA Conformation in Interpreting Infrared Spectra of Cells and Tissues. *Chem. Soc. Rev.* 2016, *45* (7), 1980–1998.

(11) Immunocytochemistry and immunofluorescence protocol | Abcam http://www.abcam.com/protocols/immunocytochemistry-immunofluorescence-protocol (accessed Oct 19, 2017).

2 Supplemental Data

2.1 MASPIN and CCN6 expression in normal breast tissue

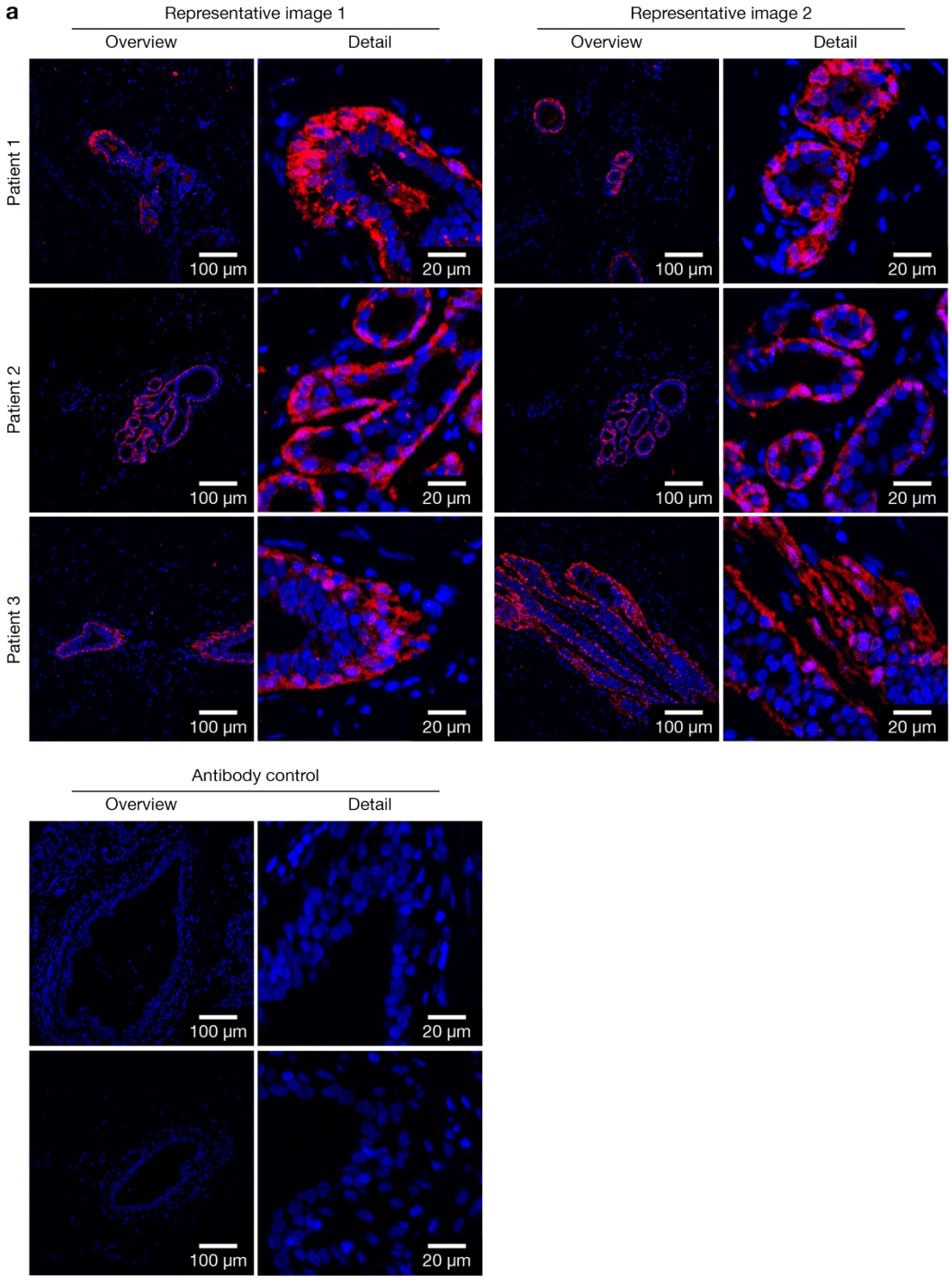

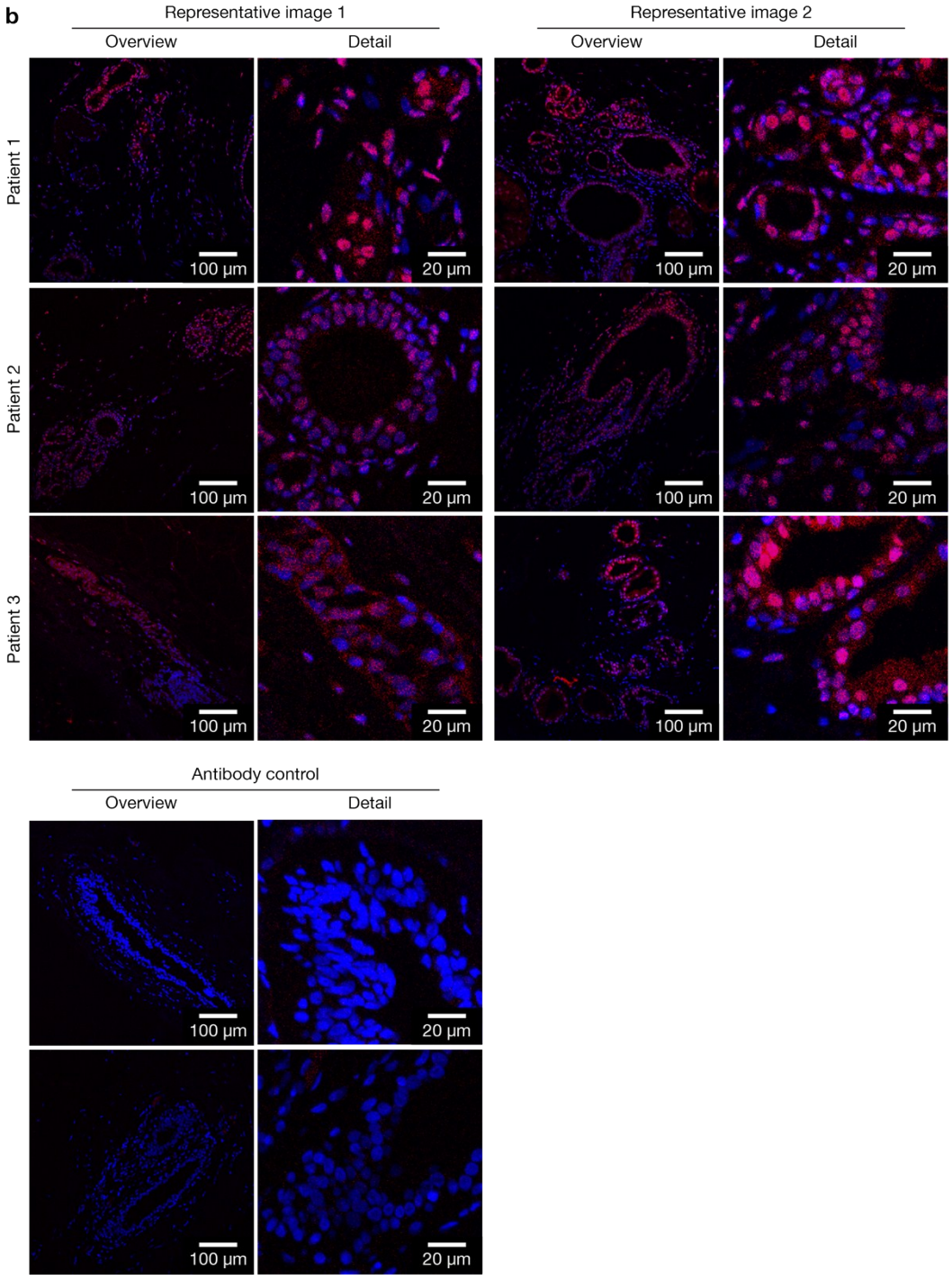
b
Representative image 1
Representative image 2
Overview
Detail
Overview
Detail
Patient 1
Patient 2
Patient 3
100 µm
20 µm
100 µm
20 µm
100 µm
20 µm
100 µm
20 µm
100 µm
20 µm
100 µm
20 µm
Antibody control
Overview
Detail
100 µm
20 µm
100 µm
20 µm

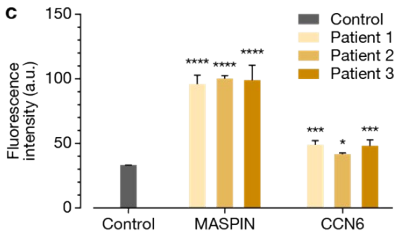

Figure S1. MASPIN (a) and CCN6 (b) expression in normal human breast tissue across 3 patients. MASPIN was expressed in normal myoepithelial cells, consistent with the literature where it is considered a normal myoepithelial marker, while CCN6 was demonstrated to be expressed in normal breast luminal epithelial cells, again consistent with previously published reports. Relative quantification of the target genes within their relative cell type is demonstrated in (c), where standard one-way ANOVA was used for statistical analysis (*$p < 0.05$, ***$p < 0.001$, ****$p < 0.0001$).

2.2 Polymer structure and characterization

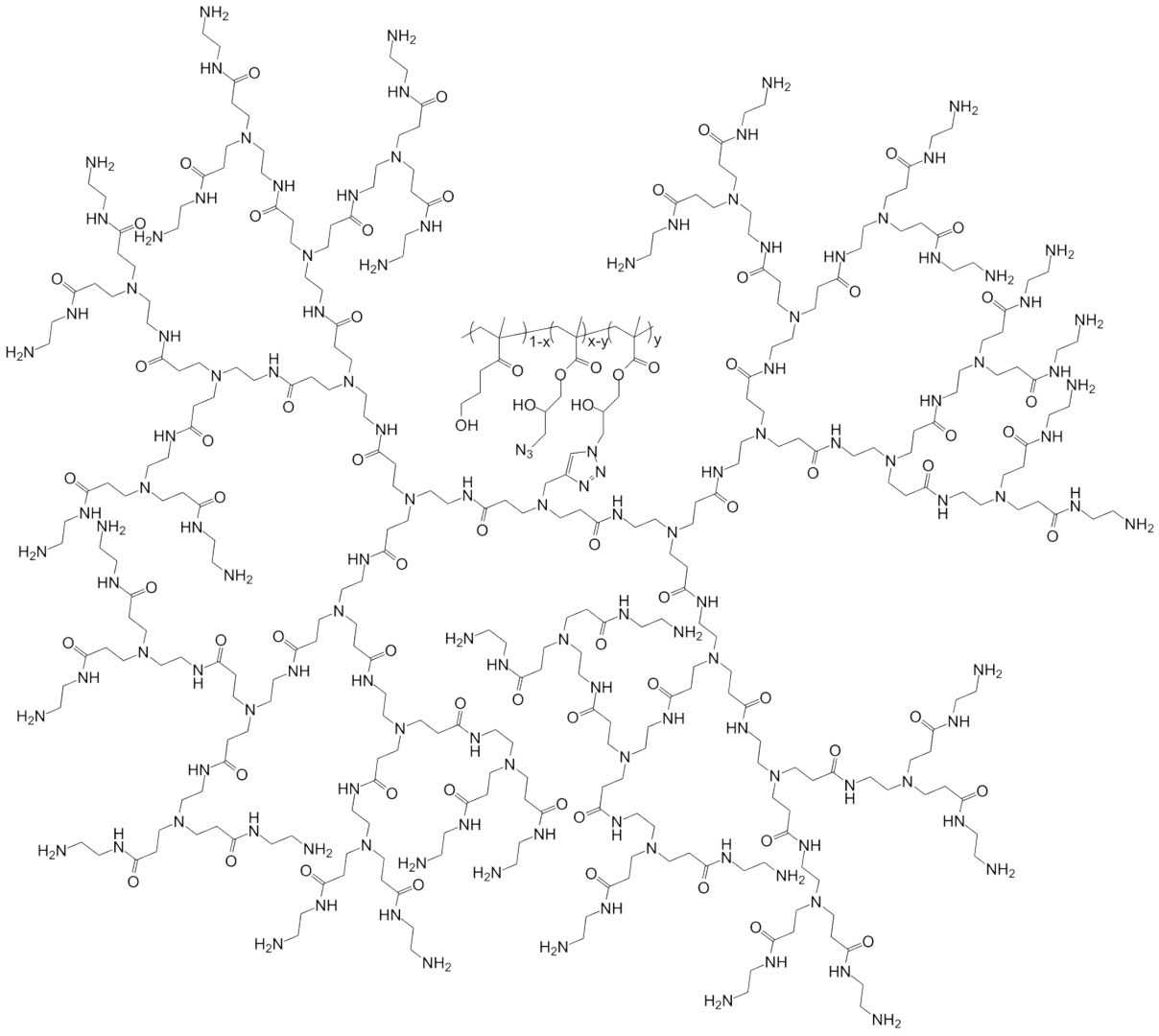

Figure S2. General structure of polymer **7**, prior to further modifications.

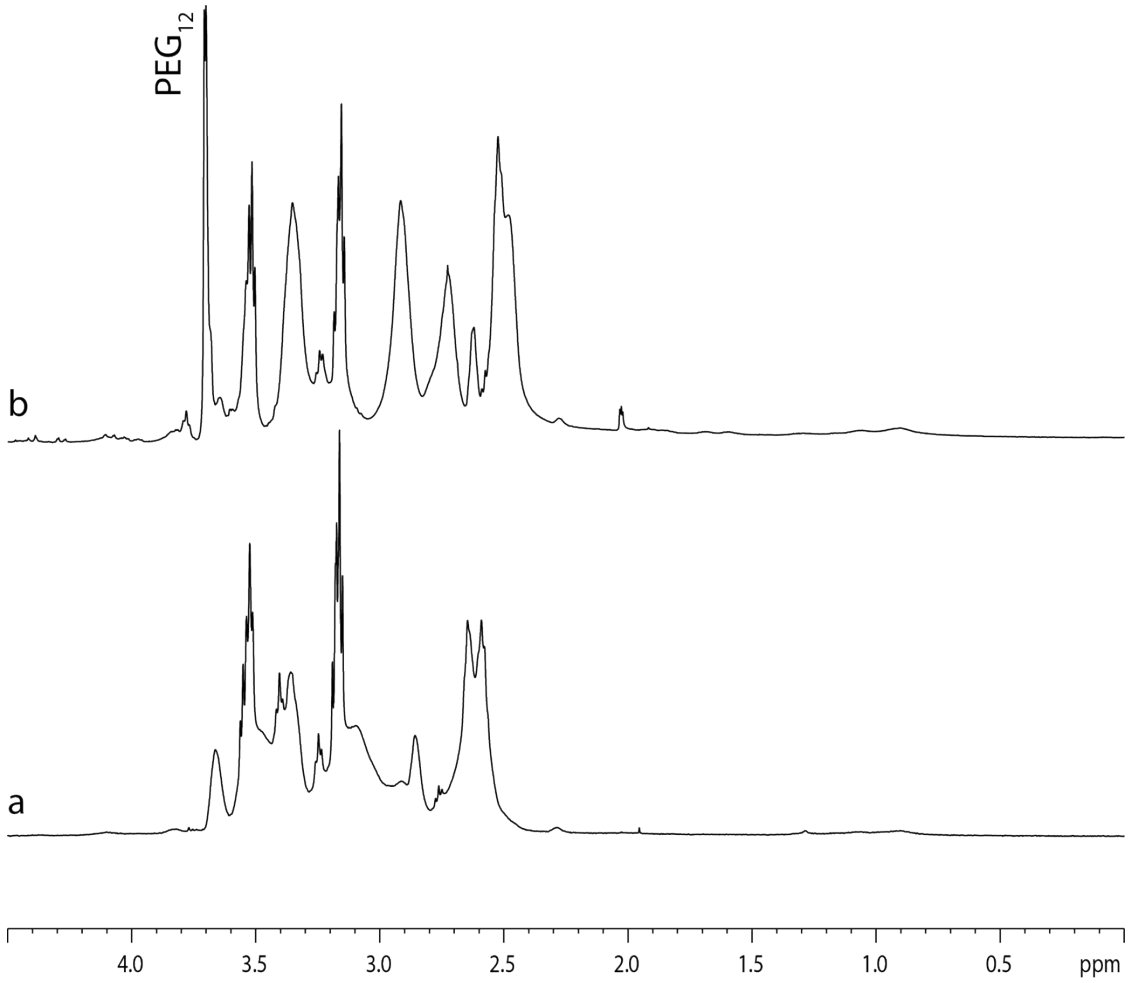

Figure S3. ^{1}H NMR spectra of polymer **7F** and **15** (a and b respectively). Spectra were taken in D_2O at 500 MHz. Peak corresponding to PEG (δ 3.79 ppm) confirms the functionalisation of polymer **7F**.

Table S5. Experimental elemental analysis of fifth generation dendron-functionalized copolymers **7** and **7F**.

Product	%C	%H	%N	%F
7	42.26; 42.47 46.31; 46.51 46.71; 46.43 (50.24)*	8.19; 7.99 8.02; 8.16 7.27; 7.62	16.07; 15.96 17.29, 17.22 17.13; 17.06 (20.77)*	-
7F	39.74; 39.79	5.43; 5.28	12.60; 12.60	23.10; 23.14

*Corrected for counter ion and water content – sample was hygroscopic; measurements were conducted three times in duplicate with repeated drying, before being normalized to average carbon percentage previously reported.

2.3 Gene regulation in H157 cells

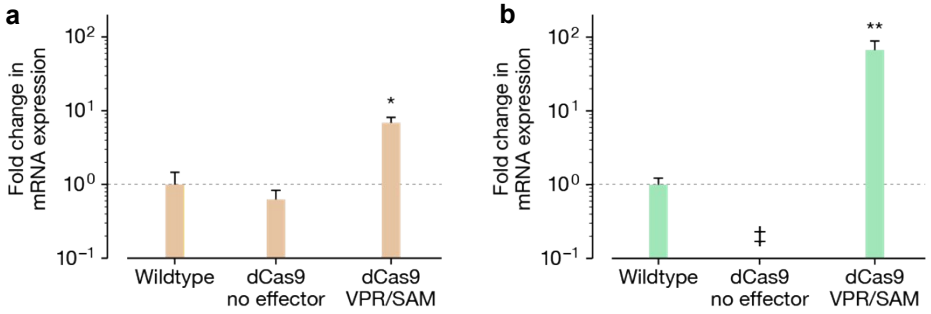

Figure S4. Transfection of H157 cells with CRISPR/dCas9 using VPR/SAM effector for the activation of MASPIN (a) and CCN6 (b). Cells were transfected with CRISPR/dCas9 no effector as a control, and normalized against wildtype. The symbol '‡' is used when signal could not be detected by qRT-PCR due to low gene expression. Data was analysed using a Students t-test, compared against wildtype cells as control, (*$p < 0.05$, **$p < 0.01$).

2.4 Off-target analysis

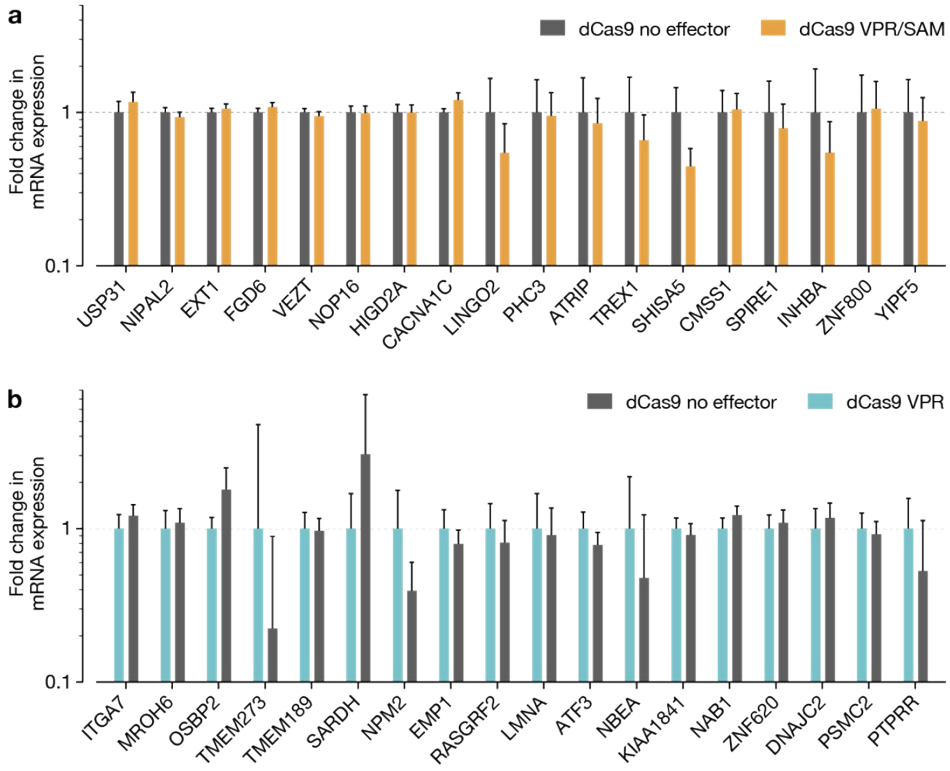

Figure S5. Off target analysis for activation of MASPIN (a) using CRISPR/dCas9-VPR/SAM and CCN6 (b) using CRISPR/dCas9-VPR. These genes represent the top 3 – 20 potential off target sites identified, with the two highest probability off-targets shown in Figure 1. None of the genes demonstrate significant variation in expression when compared to the dCas9 no effector control at 48 h post-transfection. Student's t-test was used to perform statistical analysis.

2.5 Soft agar assay

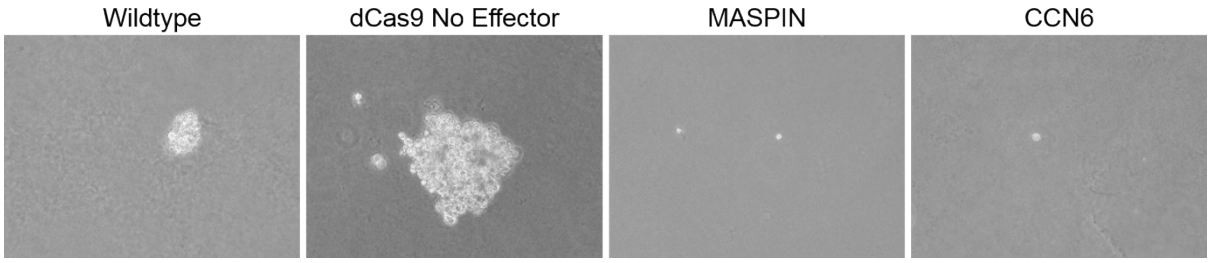

Figure S6. Representative images of colony formation in soft agar assays after 3 weeks of growth. Cells were transfected 48 h prior to being seeded for the assay.

2.6 DLS and zeta

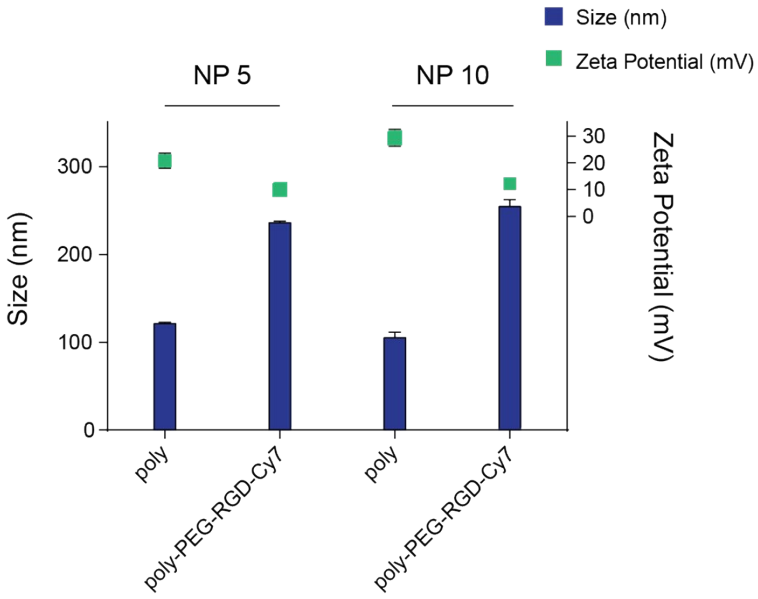

Figure S7. DLS and zeta information to assess polyplex formation for polymer (poly, **7F**) and PEG-RGD-Cy7 decorated polymer (**16**) using 5.3 kb mCherry plasmid. Binding was assessed in PBS at pH ≈ 7.4. Data shows addition of the PEG-RGD-Cy7 caused polyplex size to increase from *ca.* 100 nm to 250 nm, and charge to decrease from *ca.* +30 mV to +10 mV.

2.7 In vitro transfection of targeted polymer formulation

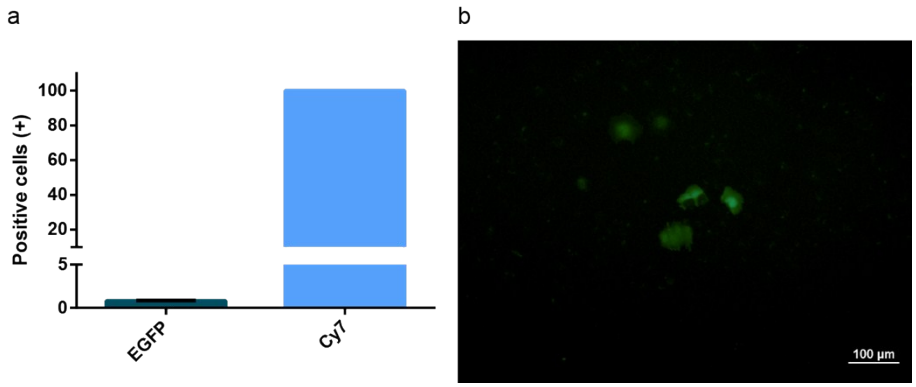

Figure S8. *In vitro* transfection check of targeted polymer formulation (poly-PEG-cRGD-Cy7) **16**, delivering EGFP. EGFP + and Cy7 + cells are given in (a), as quantified by flow cytometry. Representative fluorescent image demonstrating EGFP expression is given in (b). Transfection efficiency decreased significantly *in vitro* with the introduction of PEG-cRGD-Cy7, however cell uptake was high, recorded at 100% across n=3.

2.8 Fluorescent spectral characterisation

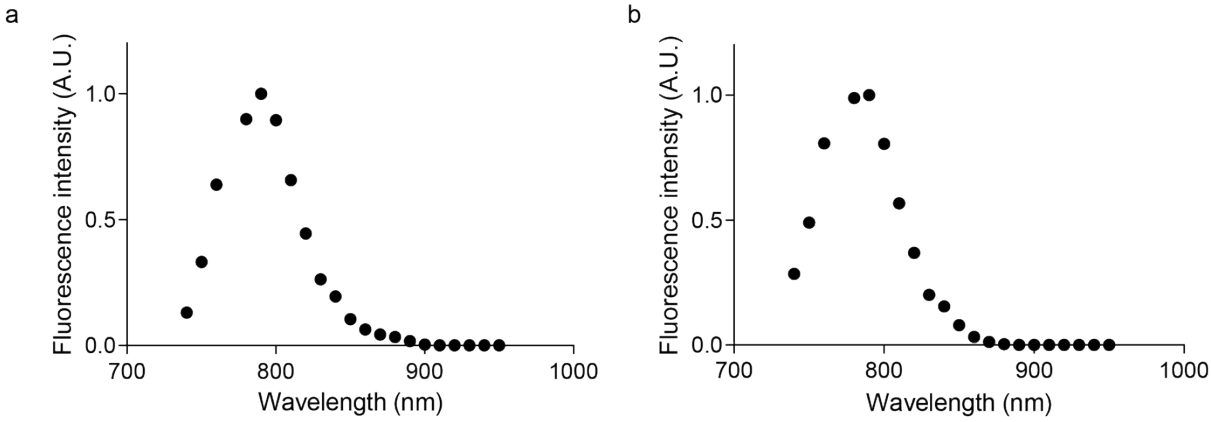

Figure S9. Spectral characterisation of non-targeted polymer **12** (poly-PEG-Cy7, a) and targeted polymer **16** (poly-PEG-cRGD-Cy7, b) for *in vivo* delivery. Both polymers demonstrated spectra with maximum emission wavelengths at ~780 nm, characteristic of Cy7, confirming the reaction, and detection using the CRi Maestro 2 imager.

2.9 Biodistribution

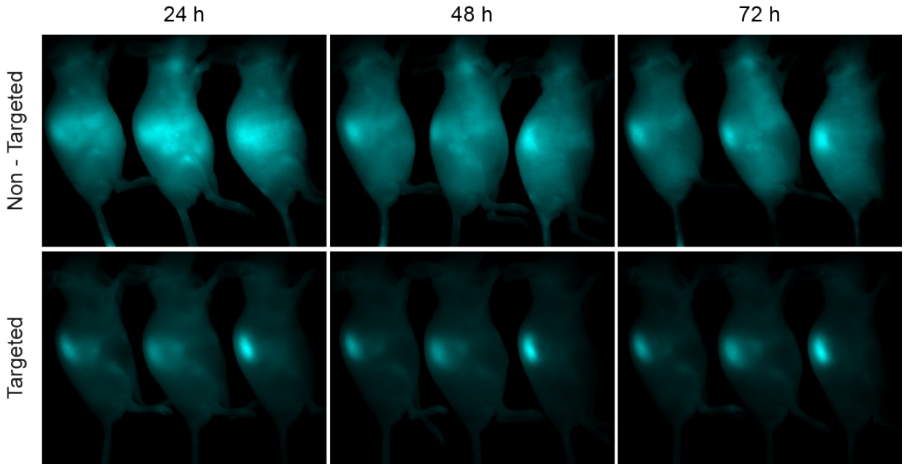

Figure S10. Unmixed whole animal in vivo multispectral imaging of Cy7-labelled polymers **12** (non-targeted) and **16** (targeted) in nude mice with MCF-7 luciferase tumour xenograft on right flank at 24 h, 48 h and 72 h. Targeted polymer **16** demonstrated high tumour uptake and clearance from kidneys, while non-targeted formulation demonstrated a longer circulation time.

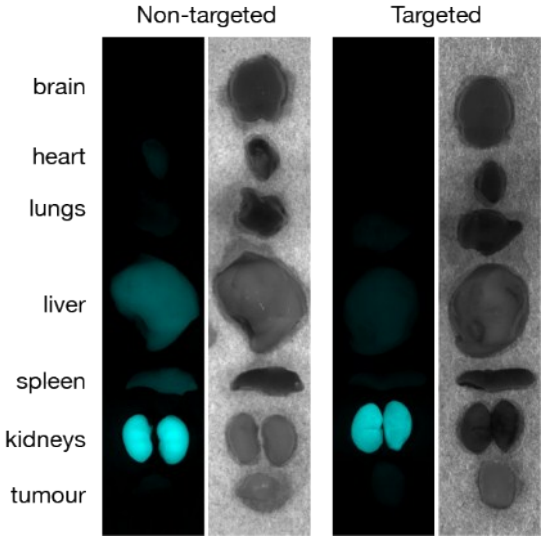

Figure S11. Unmixed *ex vivo* tissue multispectral imaging of Cy7-labelled polymers **12** (non-targeted) and **16** (targeted) showing accumulation in tissue at 72 h. Images are normalized and show relative intensities of each tissue. Photon flux of imaged *ex vivo* tissues was used to quantify total fluorescent intensity.

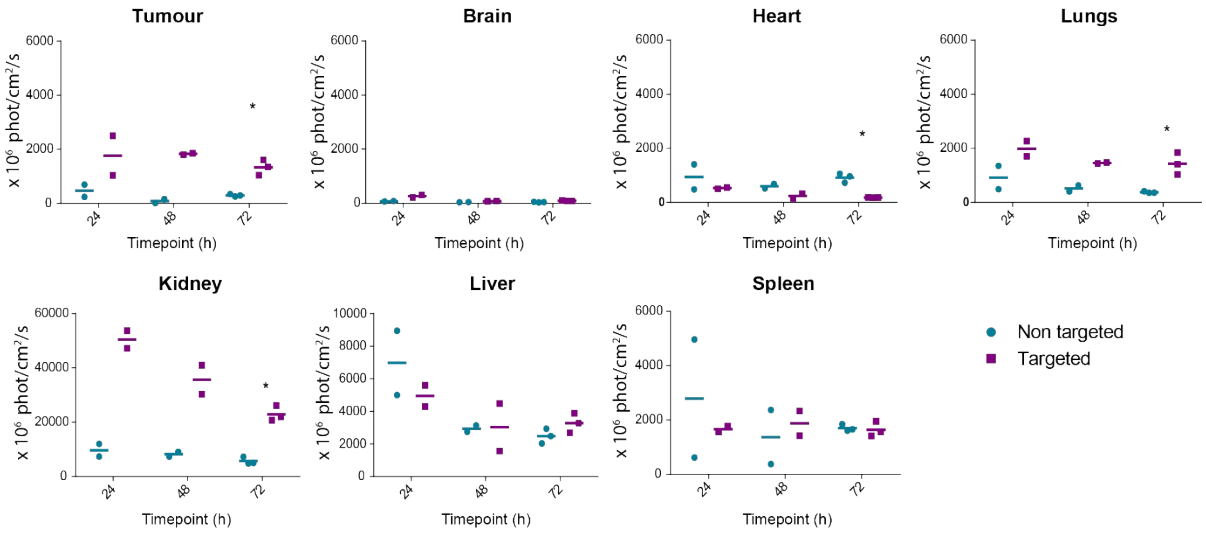

Figure S12. Average photon flux from tissue quantified from unmixed Cy7 *ex vivo* tissue images. Mice were sacrificed and imaged at 24 h and 48 h (N = 2 per condition, per time point), and at 72 h (N = 3 per condition) after single intravenous injection. Data was analysed using a Student t-test, comparing targeted against non-targeted for the appropriate tissue, as control, (*$p < 0.05$).

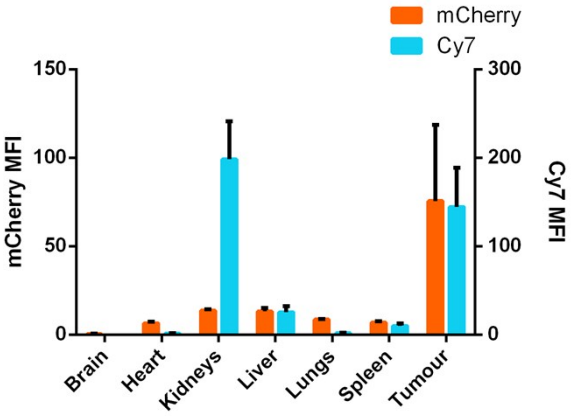

Figure S13. Mean fluorescence intensities (MFI) of mCherry and Cy7 signal in tissue harvested for flow cytometry 72 h after a single i.v. injection was administered with cRGD-targeted formulation **16**.

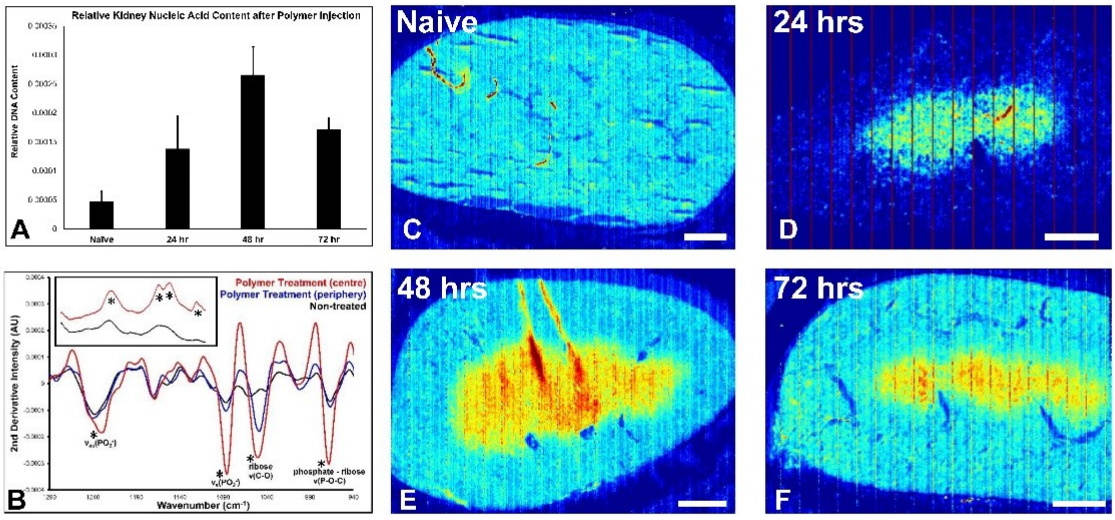

Figure S14. FTIR microscopy analysis of increased kidney nucleic acid content following injection of polymer-DNA conjugates. (A) Nucleic acid content of kidney tissue sections was found to follow a distinct time-course, increasing in the kidney following polymer-DNA conjugate injection, and reaching a maximum relative concentration at 48 hours, before being partially cleared from the tissue at 72 hours, post-injection. (B) Representative 2nd- derivative FTIR spectra from kidney tissue in the absence of, and in the presence of the polymer-DNA conjugate. A comparison of spectra taken from the centre and periphery of conjugate influx, may indicate DNA degradation. Insert shows non-derivative FTIR spectra. Asterisks indicate position of characteristic nucleic acid functional group vibrations. (C-F) Representative FTIR-microscopy functional group images of relative nucleic acid content in naïve kidney section (C), and kidney sections 24 (D), 48 (E) and 72 (F) hours after polymer-DNA conjugate injection. Scale bars = 1000 µm. Relative nucleic acid content was generated from second-derivative intensity at 1055 cm^{-1}, ribose ν(C-O). The average second-derivative intensity in panel A has been inverted, such that increasing height of the bar graph corresponds to increasing relative concentration. Error bars in panel A = standard deviation, N = 2 for naïve tissue, 24 h and 48 h, N = 3 for 72 h.

2.10 Tumour growth

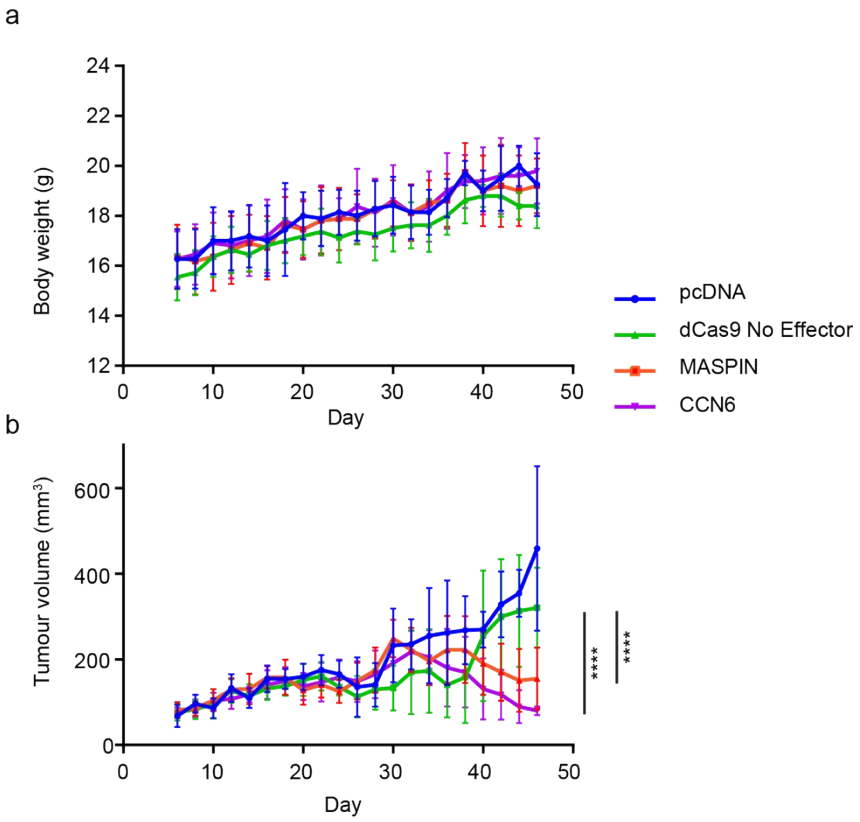

Figure S15. Body weight of BALB/c nude mice and MCF-7 luciferase xenograft tumour volume monitored throughout 46 day experiment. (a) Mice were 5 – 8 weeks old when received, body weight measurements were taken every 48 h during the course of the experiment. (b) Tumour length and width were measured every 48 h with a vernier caliper. Tumour volume was calculated as volume = 0.5 (length x width^2). Animals receiving treatments for the activation of MASPIN and CCN6 demonstrated significantly smaller tumours compared to dCas9 no effector control. Animals receiving treatment for CCN6 activation demonstrated significant tumour regression from day 30 (****$p < 0.0001$). Data was analysed using two-way ANOVA, comparing across each treatment group over time. Significance is given for the comparison of the final time point.

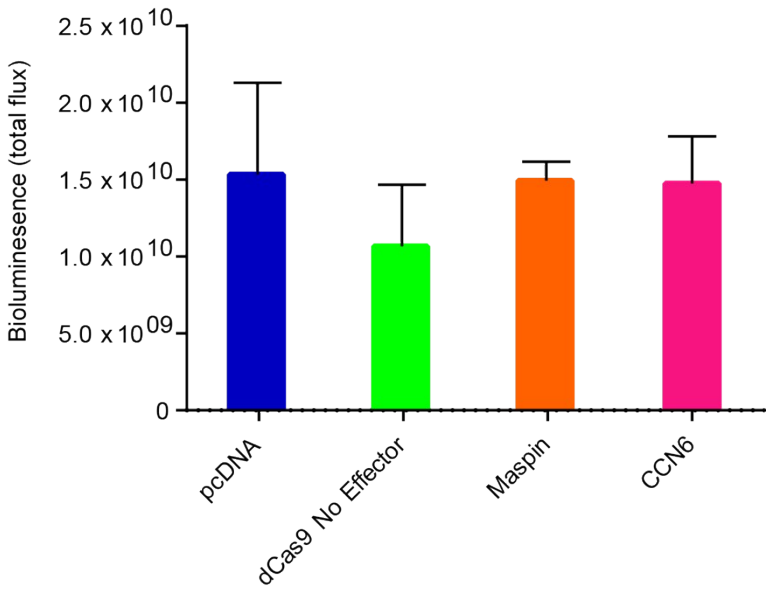

Figure S16. Bioluminescence signal of tumours on day 25, the first of the bioluminescent imaging days. Tumour size was not significantly different across groups, as assessed by multiple comparisons using a one-way ANOVA statistical analysis.

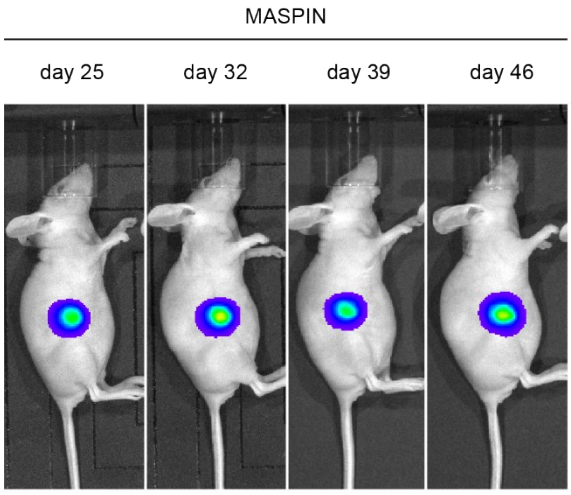

Figure S17. Representative bioluminescence images of mice treated with CRISPR/dCas9-VPR/SAM for the activation of MASPIN from day 25 to day 46.

2.11 Histology

Table S6. Histological assessment of lungs, kidneys and livers at day 23 of treatment with hematoxylin and eosin staining.

Treatment	lung	kidney	liver
pcDNA	Normal	Normal	Normal
	Normal	Normal	Normal
MASPIN	Normal	Normal	isolated necro-inflammatory foci
	mild NS changes	Normal	Normal
	Normal	Normal	isolated necro-inflammatory foci
No Effector	Normal	Normal	isolated necro-inflammatory foci
	Normal	Normal	isolated necro-inflammatory foci
	mild NS changes	Normal	isolated necro-inflammatory foci
CCN6	mild NS changes	Normal	isolated necro-inflammatory foci
	Normal	Normal	isolated necro-inflammatory foci
	Normal	Normal	isolated necro-inflammatory foci
	Acute lung injury with capillaritis	Normal	Normal

Table S7. Histological assessment of lungs and livers at day 39 of treatment with hematoxylin and eosin staining.

Treatment	lung	liver
pcDNA	mild NS changes	Normal
	mild NS changes	Normal
MASPIN	mild NS changes	isolated necro-inflammatory foci
	Normal	Normal
	Normal	Normal
No Effector	Normal	isolated necro-inflammatory foci
	Normal	Normal
	Normal	Normal
CCN6	Normal	isolated necro-inflammatory foci
	mild NS changes	isolated necro-inflammatory foci
	Normal	Normal
	mild NS changes	isolated necro-inflammatory foci

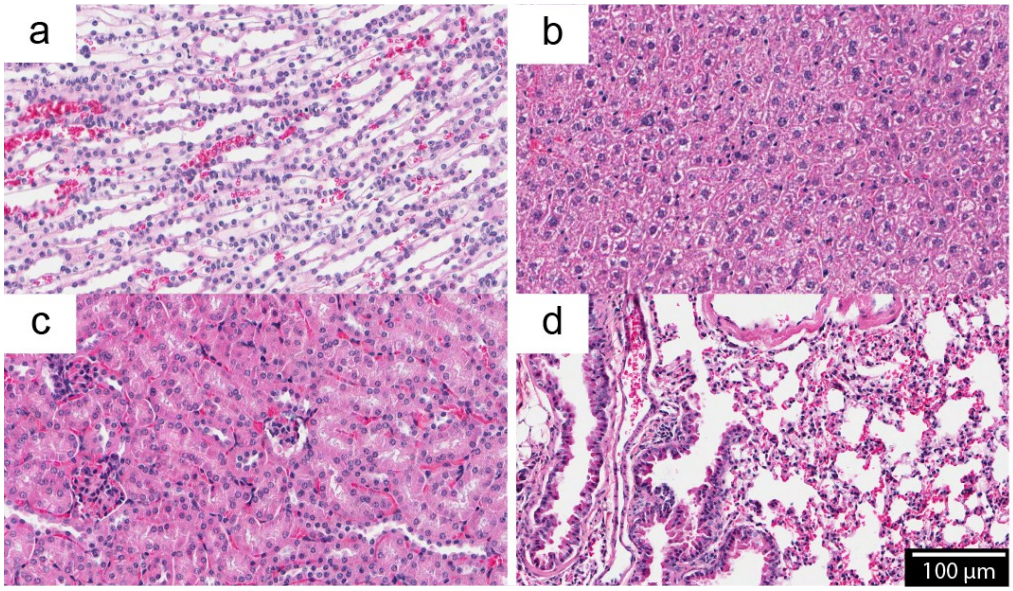

Figure S18. Representative hematoxylin/eosin stained 'normal' tissues for histological assessment. Kidney (a, c), liver (b) and lungs (d) were assessed. Samples were wax embedded for sectioning at 5 µm using a wax microtome.

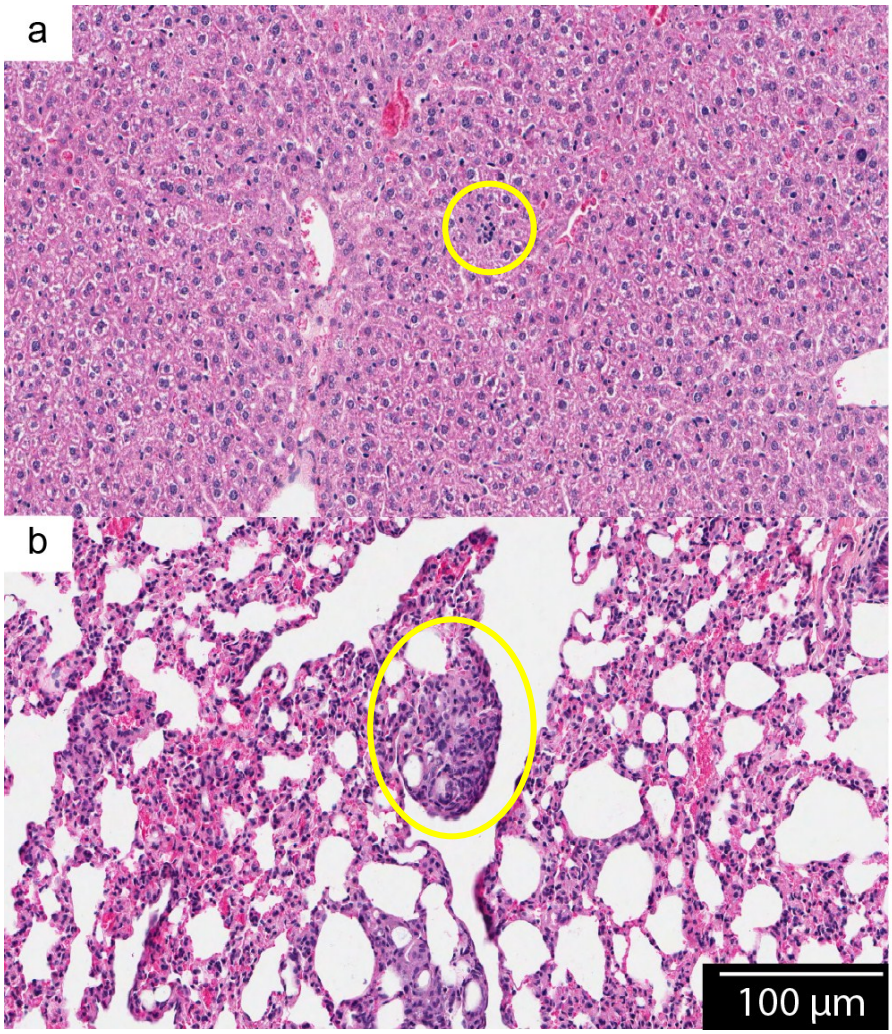

Figure S19. Representative examples of (a) non-specific inflammation in liver (isolated necro-inflammatory foci in the liver lobule) and (b) isolated non-specific granulomatous inflammation in the lungs.

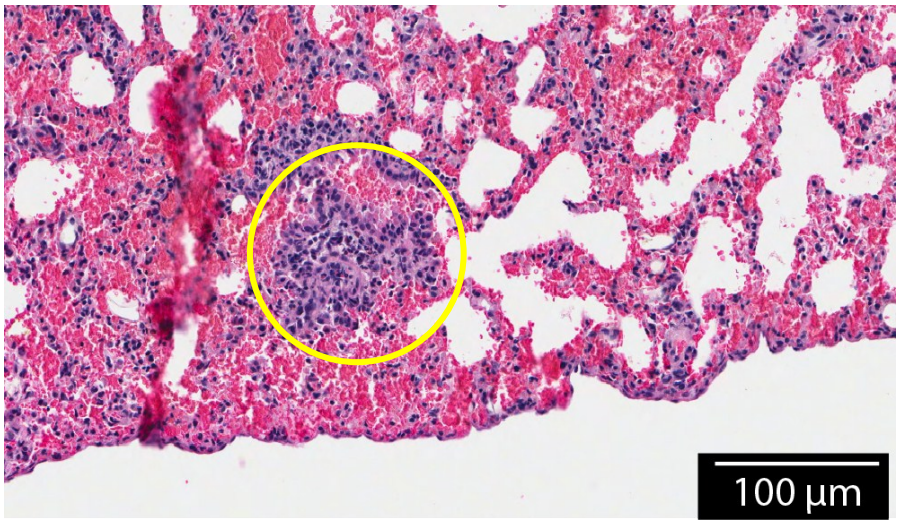

Figure S20. Acute lung injury characterised by capillaritis and surrounding haemorrhage observed in one mouse.

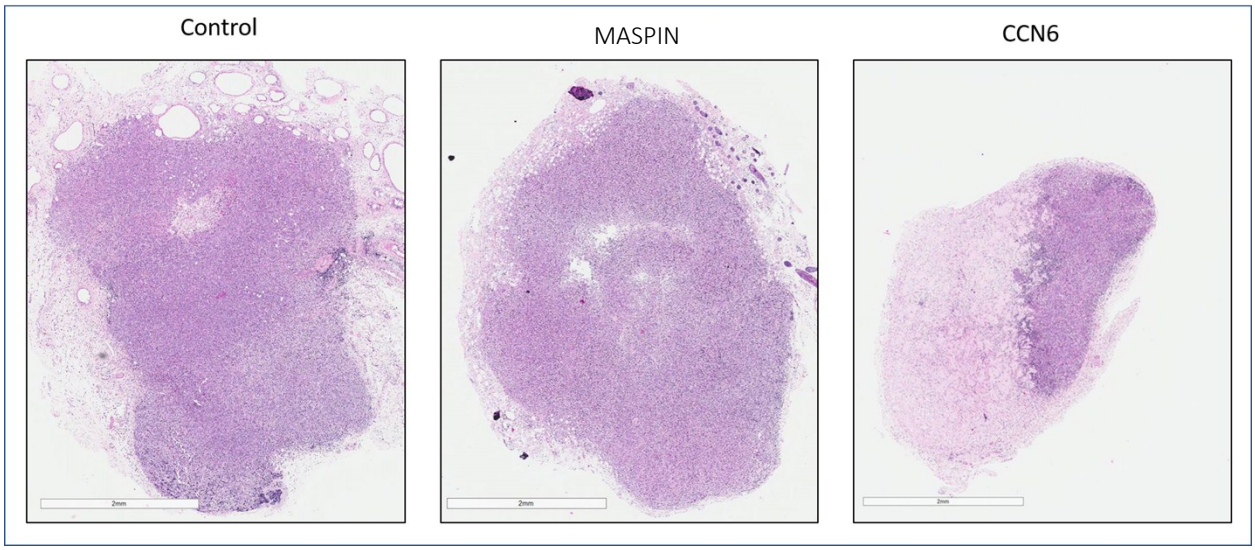

Figure S21. Selected tumours at day 46 of study with hematoxylin and eosin staining. Only the CCN6-treated tumour demonstrates tumour regression characterised by a partial fibrosis and loss of viable tumour cells.

2.12 Tissue IF

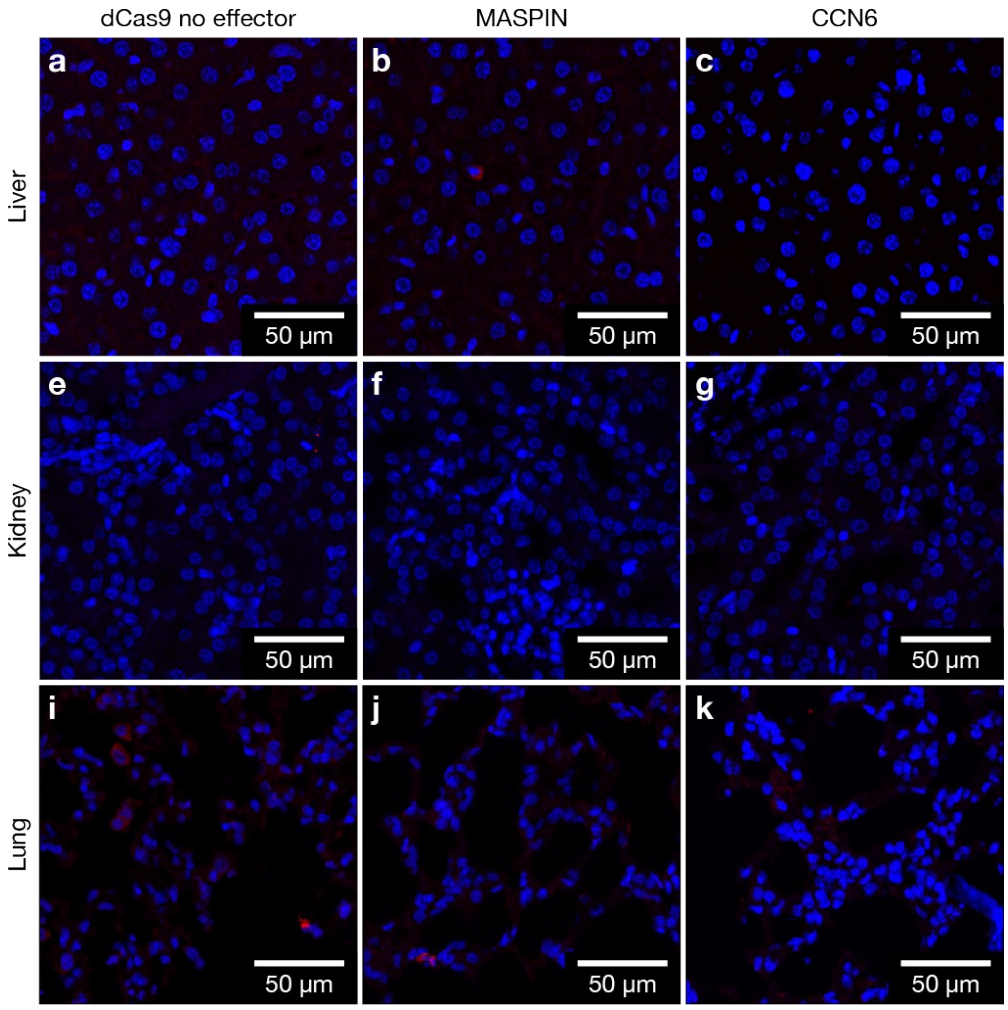

Figure S22. Immunofluorescent staining of BALB/c nude mouse tissue, including liver, kidney and lung. Tissue sections were taken from day 23 and were stained with an anti-CRISPR/Cas9 antibody to assess expression of the CRISPR/dCas9 plasmid within the cells. Across all CRISPR/dCas9 treatments (CRISPR/dCas9 no effector, and VPR/SAM and VPR targeting MASPIN and CCN6 respectively) only minimal expression was observed in the off-target tissue.

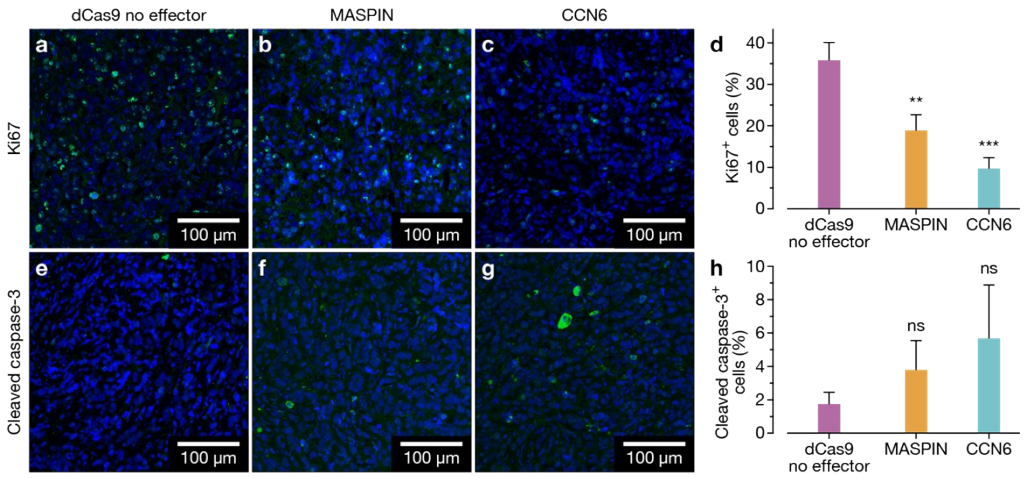

Figure S23. Immunofluorescent assessment of MCF-7-luc tumour sections at day 39. Tumour sections taken from day 39 were stained for proliferation marker Ki67 (a-c) and apoptosis marker cleaved caspase-3 (e-g). MASPIN and CCN6 upregulation caused a significant decrease in proliferation (d), however no significant different in the level of apoptosis was observed at day 39 (h). Data was analysed using a standard one-way ANOVA with multiple comparisons, (**p < 0.01, ***p < 0.005).

2.13 Guide off-targets in mouse genome

Table S8. Potential matching sequences of the human sgRNAs in the mouse genome for CCN6 (1 – 30 highest similarity).

crRNA	DNA	Chromoso-me	Position	Directi-on	Mismatc-hes	Bulge Size
CCCAGCTCAGATTCTCTCGGNGG	CCCAGtTCAGATTCTCTttGGGG	chr8	12927114	+	3	0
CCTGCCCCCGACAACGGGTGNGG	CCTGCCCCaGACcACGGGTtCGG	chr8	71380883	-	3	0
CCCAGCTCAGATTCTCTCGGNGG	CCCAGCcCAGAaTCTCTtGGAGG	chr12	7284561	+	3	0
CCCAGCTCAGATTCTCTCGGNGG	CCCAcCTgAGATTCTCTtGGAGG	chr12	94542991	-	3	0
CCTGCCCCCGACAACGGGTGNGG	CCTGCCCCCcACAgCGGGTtTGG	chr12	83921192	-	3	0
GGCCTGCACTCTGTACGTGANGG	GGCCTGCAtTCTGTcaGTGAAGG	chr12	41556644	+	3	0
CCCAGCTCAGATTCTCTCGGNGG	CCCAtCTCAGATTagCTCGGGGG	chr3	157271511	+	3	0
CCCAGCTCAGATTCTCTCGGNGG	CCCAcCTCAGATTaTCTaGGAGG	chr4	35039985	-	3	0
TCGAGAGCCTGCCATTAATANGG	TCtAGAGaCTGCCATaAATATGG	chr5	6107816	-	3	0
GGGACCCCACCCGTTGTCGGNGG	aGGACCCaACCCGTTGTaGGTGG	chr1	39629714	-	3	0
CCCAGCTCAGATTCTCTCGGNGG	CCCAtCTCAtATTCTCTCtGTGG	chr1	163606593	-	3	0

CCTGCCCCCGACAACGGGTGNGG	CaTGCCCCCtACAAgGGGTGGGG	chr2	158930421	-	3	0
GGCCTGCACTCTGTACGTGANGG	GGCtTGCAgTCTGTACGaGAAGG	chr2	103140900	-	3	0
GGCCTGCACTCTGTACGTGANGG	GGCCTGCtCTCTGTctGTGACGG	chr2	138205713	+	3	0
GGCCTGCACTCTGTACGTGANGG	GcCCTGCACTtTtTACGTGAGGG	chr19	47831410	+	3	0
GGGACCCCACCCGTTGTCGGNGG	aGGACCCCACaCcTTGTCGGTGG	chr15	45047956	-	3	0
GGGACCCCACCCGTTGTCGGNGG	aGGACCCCACCCaTTGTgGGTGG	chr15	55574381	-	3	0
CCCAGCTCAGATTCTCTCGGNGG	CtCAGCTggGATTCTCTCGGAGG	chr15	38891096	+	3	0
GGCCTGCACTCTGTACGTGANGG	GGCCTGCACaCTGgACcTGATGG	chr15	84034238	-	3	0
GGGACCCCACCCGTTGTCGGNGG	GGGACCCaACCCaTTGTgGGTGG	chr17	34252951	+	3	0
CCCAGCTCAGATTCTCTCGGNGG	CCCAGCcCAGATgCTCcCGGAGG	chr14	61314988	+	3	0
GGGACCCCACCCGTTGTCGGNGG	GGGcCCCCAtCCGTTGTgGGTGG	chrX	42494896	+	3	0
CCCAGCTCAGATTCTCTCGGNGG	CCCAGCTCAGtTTCTgTtGGCGG	chr18	55091404	+	3	0
CCCAGCTCAGATTCTCTCGGNGG	CCCAGCgCAGcTTCgCTCGGCGG	chr11	116653932	+	3	0
GGGACCCCACCCGTTGTCGGNGG	GGGACCCagCCCaTTGTgGGTGG	chr8	11856190	-	4	0
GGGACCCCACCCGTTGTCGGNGG	aGGACCCCACCCaTgGTaGGTGG	chr8	68034767	-	4	0
GGGACCCCACCCGTTGTCGGNGG	aGGACCCaACCCtTTGTgGGTGG	chr8	125603090	+	4	0
GGGACCCCACCCGTTGTCGGNGG	aGGACCCaACCCaTTGTgGGTGG	chr8	125597947	-	4	0
CCCAGCTCAGATTCTCTCGGNGG	CCCAGCTCAGgTTtTCTtGtGGG	chr8	4199570	+	4	0
CCCAGCTCAGATTCTCTCGGNGG	CCaAGCTCAcATTCcCTtGGAGG	chr8	10803994	-	4	0

Table S9. Potential matching sequences of the human sgRNAs in the mouse genome for MASPIN (1 – 30 highest similarity).

crRNA	DNA	Chromoso-me	Position	Directi-on	Mismatc-hes	Bulge Size
GATGTGGAGGCGACCGTGTCNGG	GATGTGGAGGtGACtGTGTCAGG	chr9	31088715	-	2	0
GTAGGAGAGGAGTGCCGCCGNGG	GgAGGAGAaGgGTGCCGCCGGGG	chr8	119505572	-	3	0
GTAGGAGAGGAGTGCCGCCGNGG	GaAGGAGAGGAGTGCCaCCcAGG	chr3	107237097	-	3	0
GGCCTCCAACATGTTCGGGCNGG	GGCCTCCAgCATGTTaGGGaGGG	chr7	110627833	+	3	0
GTAGGAGAGGAGTGCCGCCGNGG	GcAGGAGAGGAGaGCtGCCGTGG	chr4	11726845	+	3	0
GGCCTCCAACATGTTCGGGCNGG	GGCCTtgAACATGTTgGGGCAGG	chr5	47410068	+	3	0
GGCCTCCAACATGTTCGGGCNGG	GtCCTCCtACATGTTCtGGCAGG	chr2	109159136	-	3	0
GTAGGAGAGGAGTGCCGCCGNGG	GTAGGAGAGGtGgGCaGCCGAGG	chr10	93972468	+	3	0
GGCCTCCAACATGTTCGGGCN	GGgCTCCAgCATGTTCaGGCA	chr10	53889667	-	3	0

GG	GG						
GGCCTCCAACATGTTCGGGCNGG	GGtgTCCAACATGTTCGGGtTGG	chr6	31055673	+	3	0
GATGTGGAGGCGACCGTGTCNGG	GATGTGGgGGCGAgCaTGTCTGG	chr14	67819140	-	3	0
GATGTGGAGGCGACCGTGTCNGG	GATagGGAGGCGACCGTGaCAGG	chr18	53372358	+	3	0
GGCCTCCAACATGTTCGGGCNGG	GGCCTCCAAaATGTTaGaGCAGG	chr11	4963815	+	3	0
GTAGGAGAGGAGTGCCGCCGNGG	GgAGGAGAGcAGTGCgcCCGCGG	chr8	25754347	+	4	0
GTAGGAGAGGAGTGCCGCCGNGG	GTAGcAGAGGAcTGCCtCaGTGG	chr8	30810047	+	4	0
GTAGGAGAGGAGTGCCGCCGNGG	GTAGGgGAGGAGTGCCaggGGGG	chr8	68698074	+	4	0
GTAGGAGAGGAGTGCCGCCGNGG	GcAGGAGAGGAGaGCtGCCaTGG	chr8	80108895	+	4	0
GTAGGAGAGGAGTGCCGCCGNGG	GcAGGAGAGGAGaGCtGCCcTGG	chr8	94474004	+	4	0
GATGTGGAGGCGACCGTGTCNGG	aATGTGGAGGaGAgaGTGTCAGG	chr8	27053246	-	4	0
GATGTGGAGGCGACCGTGTCNGG	GgaGTGGAGGCGAgCaTGTCAGG	chr8	32908507	-	4	0
GATGTGGAGGCGACCGTGTCNGG	cATGgGcAGGCaACCGTGTCAGG	chr8	75081478	-	4	0
GCAATCCTCTCGGCCCACGCNGG	GCtAgCCTCTCaGCCCACGaGGG	chr8	60860952	+	4	0
GCAATCCTCTCGGCCCACGCNGG	GCcATCCTCTgGGCCCACagTGG	chr8	106866991	+	4	0
GCAATCCTCTCGGCCCACGCNGG	tCAAaCCTCTCtGgCCACGCTGG	chr8	109595640	+	4	0
GCAATCCTCTCGGCCCACGCNGG	GCAcTgCTCTtGGCCCACGtTGG	chr8	126619294	+	4	0
GGCCTCCAACATGTTCGGGCNGG	GGtCTgCAACATGTTCacGCTGG	chr8	31360432	+	4	0
GGCCTCCAACATGTTCGGGCNGG	GGCaTCCAACATGTcCctGCGGG	chr8	34817178	-	4	0
GGCCTCCAACATGTTCGGGCNGG	GGaCTCCAAttTGTTgGGGCCGG	chr8	75245022	-	4	0
GGCCTCCAACATGTTCGGGCNGG	GGCCTCCAACAgtTgCGGGtTGG	chr8	87621520	+	4	0
GGCCTCCAACATGTTCGGGCNGG	GGCCTCCAACATGcTaGGcaAGG	chr8	117271239	-	4	0

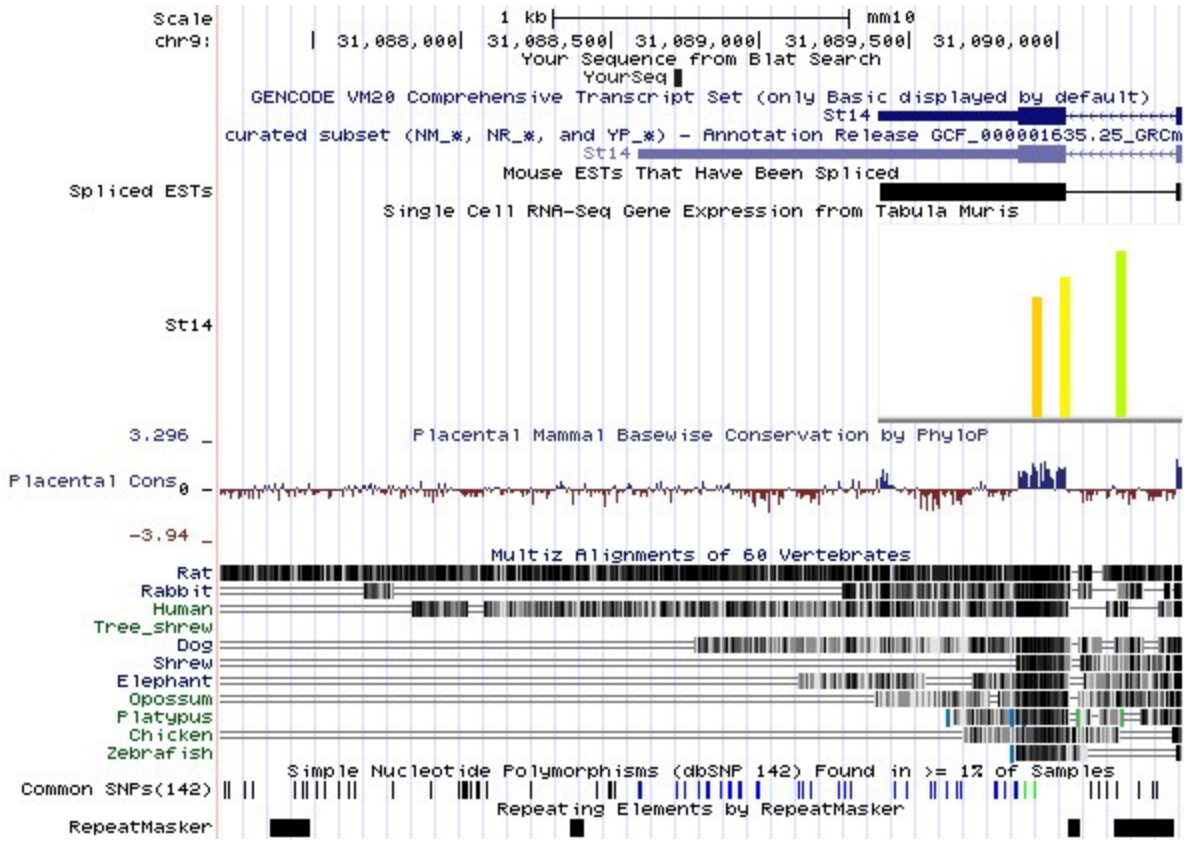

Figure S24. Positioning of sequence in mouse genome with the highest similarity of a MASPIN-specific sgRNA used in this study. The sequence has 2 mismatches, and does not reside within an annotated promoter region.